Inverse Dynamics Analysis of Human Walking

A Project Report

submitted by

ABHYUDIT SINGH MANHAS

in partial fulfilment of the requirements

for the award of the degree of

BACHELOR OF TECHNOLOGY

DEPARTMENT OF MECHANICAL ENGINEERING
INDIAN INSTITUTE OF TECHNOLOGY MADRAS.

May 2022

THESIS CERTIFICATE

This is to certify that the thesis titled **Inverse Dynamics Analysis of Human Walking**, submitted by **Abhyudit Singh Manhas**, to the Indian Institute of Technology, Madras, for the award of the degree of **Bachelor of Technology in Mechanical Engineering**, is a bona fide record of the research work done by him under the supervision of **Dr. Sourav Rakshit** during the academic year 2021-22. The contents of this thesis, in full or in parts, have not been submitted to any other Institute or University for the award of any degree or diploma.

Dr. Sourav Rakshit
Research Guide
Assistant Professor
Dept. of Mechanical Engineering
IIT Madras, 600036

Place: Chennai
Date: 27th May 2022

ACKNOWLEDGEMENTS

I would like to express my sincere gratitude to my guide Dr. Sourav Rakshit for providing his invaluable guidance, comments and suggestions throughout the course of the project. He let me work at my own pace along my own lines, while providing me with useful directions whenever necessary.

I would also like to thank Mr. Mowbray Rajagopalan for providing me with data required to complete my analyses.

ABSTRACT

KEYWORDS: Biomechanics, Multi-Body dynamics, Inverse kinematics, Inverse Dynamics

Many spinal cord injury and stroke patients lose their ability to walk. Exoskeletons are wearable devices that help them in regaining this ability by applying moments corresponding to normal walking at their joints. This warrants an inverse dynamics analysis for normal and healthy walking, in order to estimate these joint moments. Such an analysis typically requires kinematic data and data about the ground reaction forces (GRF). Thus in this project, various inverse dynamics models have been investigated, in both 2D and 3D, and joint moments have been computed.

We initially look at models where the GRF is known, and then address the situation when data about the GRF might be unavailable. For this, we present a novel formulation in which the GRF is estimated from a 2D whole body lagrangian analysis and the zero-moment point (ZMP) concept. We also try to estimate the GRF by utilizing the ZMP concept for a 3D whole body analysis. Once the joint moments have been computed, the motors of the exoskeleton can then apply these values of moments to correct the gait of a patient.

TABLE OF CONTENTS

ABBREVIATIONS

SCI	Spinal cord injury
GRF	Ground reaction forces
CoM	Centre of mass
ZMP	Zero-moment point
DH	Denavit-Hartenburg
DOF	Degree(s) of freedom
BWS	Body weight support
AP	Anteroposterior
ML	Mediolateral
FBD	Free-body-diagram

CHAPTER 1

INTRODUCTION

Every year, around $2,50,000$ to $5,00,000$ people suffer from spinal cord injuries globally. Spinal cord injuries (SCI) could be caused by falls, motor vehicle accidents, sports injuries, diving accidents, violence, infections or birth injuries. Symptoms of a SCI can vary widely. The location of the injury on the spinal cord determines what part of the body is affected and how severe the symptoms are. Generally, the higher up the level of the injury to the spinal cord, the more severe are the symptoms. In most cases, there is muscle weakness and loss of voluntary muscle movement and sensation in the chest, arms, or legs. People who suffer from significant spinal injuries can find themselves unable to walk because they can no longer control their legs as they did before.

A stroke happens when blood flow to a part of the brain is cut off. Without the oxygen in blood, brain cells start dying within minutes. Annually, around 15 million people worldwide suffer a stroke. Of these, about 5 million die and another 5 million are left permanently disabled. It is estimated that around 1 in 4 adults over the age of 25 will have a stroke in their lifetime. A stroke is usually caused by high blood pressure, excessive smoking, diabetes, heart disease, obesity, or excessive alcohol intake. The majority of strokes injure the motor fibers connected to movement. They typically damage portions of one side of the brain and affect the opposite side of the body. A stroke can make one side of the body weak or paralyzed, making it difficult or impossible to walk. A stroke patient may also experience a complete lack of sensation in parts of the body. A patient's balance may also be shaky, if the cerebellum is injured. And along with the paralysis, weakness, numbness, and loss of balance, many stroke patients are left with distorted perceptions about where the body ends.

Thus, many SCI and stroke patients find it very difficult to walk. For these patients, active rehabilitation training should be started as early as possible, so that they can regain their ability to walk normally, to some extent. Lower limb exoskeleton robots are greatly useful for this purpose, as they reduce the burden on

therapists, realize data detection during training, and aid the quantitative evaluation of recovery in a controllable and repeatable manner. Lower limb rehabilitation exoskeleton robots integrate sensing, control, and other technologies and exhibit the characteristics of bionics, robotics, information and control science, medicine, and other interdisciplinary areas. They connect with the patient's body/limbs in a wearable way and can control the movement of all joints in the training process, which can simulate normal walking/gait and drive the patient's limb to realize exoskeleton-assisted rehabilitation training. In our situation, the patients will receive gait training from a treadmill-based exoskeleton robot on a treadmill. In such a robot, in addition to the exoskeleton that is used to provide assistance to leg movement, there is a body weight support (BWS) system, which is required to reduce gravitational forces acting on the legs, ensure safety, and maintain balance. Therefore for the purpose of rehabilitation, it is imperative that the exoskeleton applies the correct values of forces and moments at the joints, so that it corresponds to normal walking. The question is how can these joint forces and moments be estimated ? They can be estimated by an inverse dynamics analysis. In inverse dynamics, we require (i) kinematic/gait data (ii) external forces (if available), and (iii) data about masses of the body segments and locations of their centre of mass, to compute joint forces and moments. Once these forces and moments are calculated, they are inputted to the motors of the exoskeleton, which then apply it to the joints of the patient, aiding in rehabilitation. In the next chapter, a quick summary on human gait analysis is presented, before moving onto the different inverse dynamics models.

CHAPTER 2

HUMAN GAIT ANALYSIS

The human walking process is mainly accomplished by lower limbs, and hence, analyzing their structure and movement characteristics is necessary. Walking is achieved by coordination between the pelvis, hip, knee, and ankle. The pelvis is located between the trunk and the thighs. The hip joint, which is a ball-and-socket joint, is formed by the femoral head and the acetabulum of the pelvis, and it allows simultaneous movement between the thighs and pelvis. It allows flexion and extension in the sagittal plane, abduction and adduction in the frontal plane, and internal and external rotation in the transverse plane. The knee is a joint complex containing tibiofemoral and patellofemoral joints. Their movement occurs in two planes, allowing flexion and extension in the sagittal plane, and internal and external rotation in the transverse plane. During walking, the knees perform some important functions. In the swing phase, knees shorten leg length by flexion. In the stance phase, they remain flexed to absorb shock and transmit forces through legs. The ankle/foot is a complex structure that absorbs this shock and imparts thrust to the body. The ankle movements mainly occur about talocrural and subtalar joints. The talocrural joint is located between the talus, distal tibia, and fibula to provide plantarflexion and dorsiflexion (in the sagittal plane) as a hinge joint, in which the surface of one bone is spool-like and the surface of the other bone is concave. The subtalar joint is located between the calcaneus and talus and allows eversion and inversion (in the frontal plane) and internal and external rotation (in the transverse plane). The basis for the mechanical design of rehabilitation exoskeleton robots is provided by an analysis of the lower limb structure.

As mentioned previously, kinematic data is a very important requirement for an inverse dynamics analysis. Kinematic data is usually collected by the use of human motion capture systems. Human motion capture systems are used in various fields to analyse, understand and reproduce the diversity of movements that are required during daily-life activities. In our situation, we use it to obtain the

kinematic/gait data for a healthy individual. There are many online repositories available that contain gait data for healthy individuals. For our analysis, we take it from [5]. Schreiber and Moissenet have collected gait data for 50 healthy individuals. They define a participant to be healthy if they are injury free in both lower and upper extremities in the most recent six months, and have had no lower or upper extremity surgery in the last two years. For every participant, they have recorded the gait data for 5 different conditions of walking speed: between 0 and 0.4 m/s, between 0.4 and 0.8 m/s, between 0.8 and 1.2 m/s, a self-selected spontaneous speed, and a self-selected fast speed. The last two walking speeds were self-selected conditions in response to the instructions to walk respectively "as usual" and "fast but not running". We consider the gait data of a random healthy participant, corresponding to the fourth condition of walking speed, as it is the closest to a self-selected natural walking speed.

The kinematic data was recorded by placing 52 cutaneous reflective markers on the participant's body, and then tracking their three-dimensional (3D) trajectories using a 10-camera optoelectronic system sampled at 100 Hz. The markers were placed by anatomical palpation on the participant, and are shown in figure 2.1.

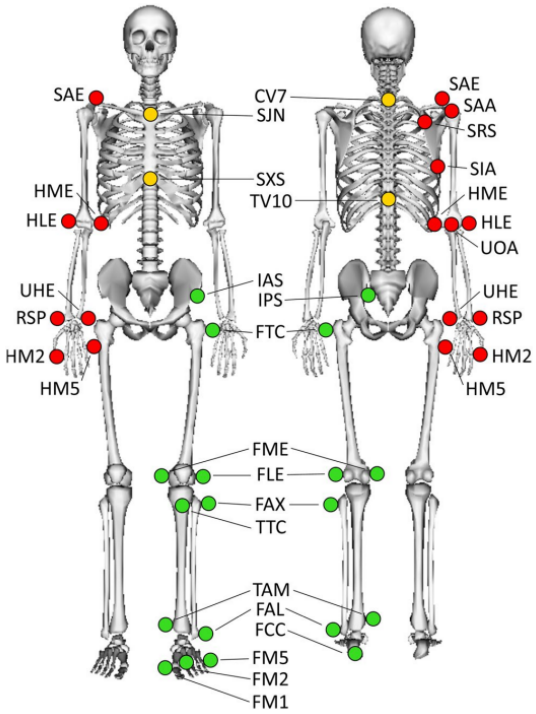

Figure 2.1: Markers on the participant. The green markers correspond to the left side of the lower limbs, and the red markers correspond to the right side of the upper limbs (adapted from [5]).

We are mainly interested in the lower limbs of the body, and so the anatomical landmarks of the markers are presented in table 2.1.

Table 2.1: Anatomical landmarks of the relevant markers.

Labels	Unit	Description
SXS	mm	Suprasternal notch coordinates
L_FTC	mm	Left greater trochanter coordinates
L_FLE	mm	Left lateral femoral epicondyle coordinates
L_FME	mm	Left medial femoral epicondyle coordinates
L_FAL	mm	Left lateral tibial malleolus coordinates
L_TAM	mm	Left medial tibial malleolus coordinates
L_FCC	mm	Left posterior calcaneus coordinates
L_FM2	mm	Left 2nd metatarsal head coordinates
R_FTC	mm	Right greater trochanter coordinates
R_FLE	mm	Right lateral femoral epicondyle coordinates
R_FME	mm	Right medial femoral epicondyle coordinates
R_FAL	mm	Right lateral tibial malleolus coordinates
R_TAM	mm	Right medial tibial malleolus coordinates
R_FCC	mm	Right posterior calcaneus coordinates
R_FM2	mm	Right 2nd metatarsal head coordinates

All the marker trajectories are stored in a .c3d file, and then imported and processed under MATLAB, using the Biomechanics ToolKit. For our analysis, the SXS marker corresponds to the trunk. The L_FTC marker corresponds to the left hip. The mid point of the L_FLE and L_FME markers corresponds to the left knee. The mid point of the L_FAL and L_TAM markers corresponds to the left ankle. The L_FCC marker corresponds to the heel of the left foot, and the L_FM2 marker corresponds to the left forefoot. Similarly, the R_FTC marker corresponds to the right hip, the mid point of the R_FLE and R_FME markers corresponds to the right knee, the mid point of the R_FAL and R_TAM markers corresponds to the right ankle, the R_FCC marker corresponds to the heel of the right foot, and the R_FM2 marker corresponds to the right forefoot.

As stated earlier, another requirement for an inverse dynamics analysis is the data about masses of the body segments and locations of their centre of mass (CoM), also known as body segment parameters. This is usually available as anthropometric data, and no separate measurements need to be done for this.

The other requirement for an inverse dynamics analysis is the data on external forces. The external forces acting on the participant/system are gravity and the ground reaction force (GRF). Since the mass of each body segment is known, the gravity force acting on each segment is also known. To measure the GRF, we usually require force plates. However, the GRF can also be estimated using the kinematic data and body segment parameters alone, but this will be discussed later (in sections 3.4 and 3.5). Two force plates sampled at 1500 Hz were used to record the 3D ground reaction force and moment. These force plates were embedded in the middle of the walkway travelled during the overground walking trials. All measurements start from 0 sec, end at 2.12 sec, and are made at 0.01 sec time intervals. It is also important to designate the different events of the gait cycle, and mention the times at which they occur. The double stance phase is the period when both the legs are in contact with the ground. The left leg single stance phase is the period when only the left leg is in contact with the ground, and it corresponds to the right leg swing phase, i.e. when the right leg swings to advance the CoM of the body. Similarly, we have a right leg single stance phase, which corresponds to the left leg swing phase. One gait cycle has two single stance phases, and two double stance phases. For more information about the gait cycle and the different events that occur, one can consult [3] or [9].

For the healthy candidate chosen, the right leg swing phase/left leg single stance phase lasts from 0.23 sec to 0.75 sec. The first double stance phase lasts from 0.76 sec to 0.9 sec. The left leg swing phase/right leg single stance phase lasts from 0.91 sec to 1.43 sec. Finally, the second double stance phase lasts from 1.44 sec to 1.58 sec. This is summarized in table 2.2.

Table 2.2: Duration of different phases of the gait cycle.

Phase	Duration
Right leg swing/left leg single stance phase	0.23 s to 0.75 s
First double stance phase	0.76 s to 0.9 s
Left leg swing/right leg single stance phase	0.91 s to 1.43 s
Second double stance phase	1.44 s to 1.58 s

Thus, one gait cycle starts at 0.23 sec, ends at 1.58 sec, and lasts for 1.35 seconds. Walking in general can be considered to be an activity in three dimensions. Let the x-axis be in the direction of walking, and the y-axis be vertically upward. That is, the x-axis is along the anteroposterior or AP axis, the y-axis is along the longitudinal axis, and the z-axis is along the mediolateral or ML axis. Let the components of the experimental/measured ground reaction force along these axes be denoted by GRF_x, GRF_y and GRF_z respectively. The plots of the these components versus time, for the right leg, are shown in figures 2.2 to 2.4.

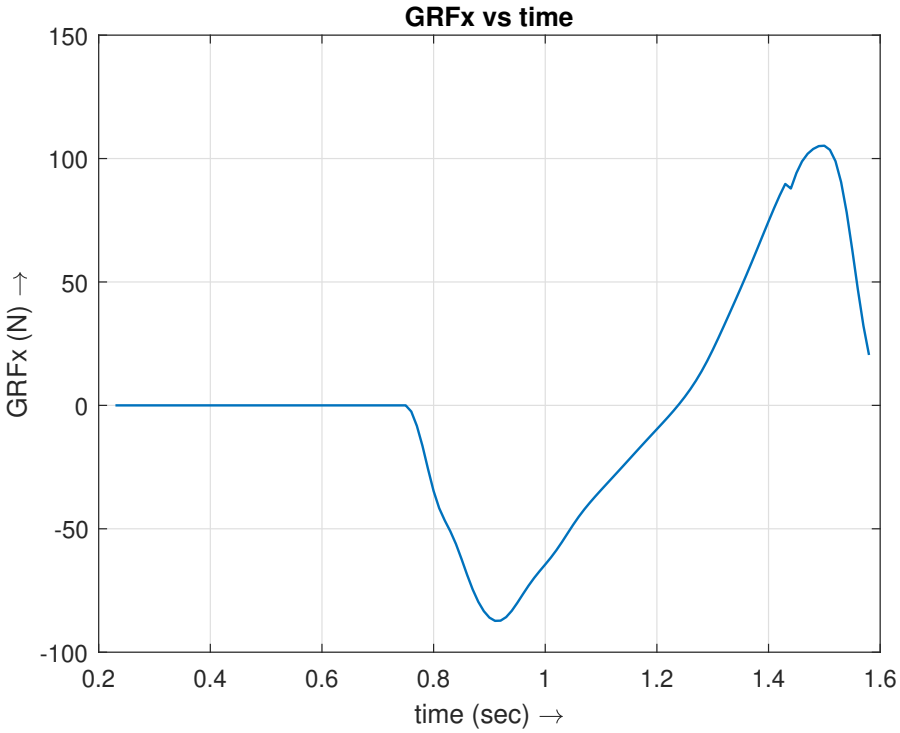

Figure 2.2: Variation of GRF_x versus time

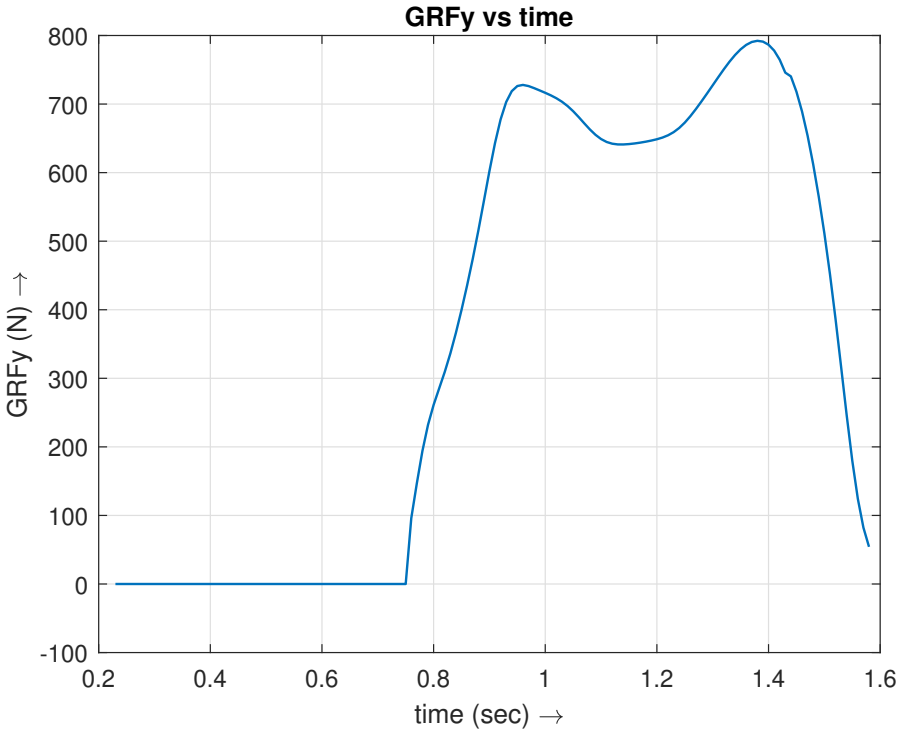

Figure 2.3: Variation of GRF_y versus time

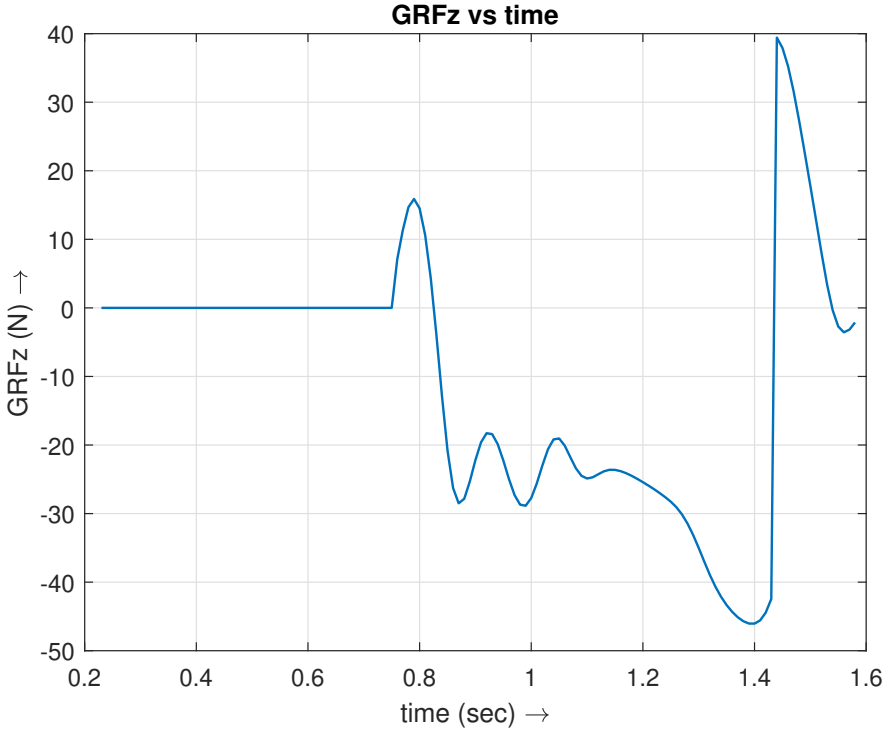

Figure 2.4: Variation of GRF_z versus time

Initially, the value of GRF_x is zero, as the right leg is in swing phase. The foot of the right leg then contacts the ground at the end of the swing phase, and decelerates to rest. Thus, GRF_x or the frictional force acts in the negative x

direction, i.e. opposite to the direction of walking. Then towards the end of the stance phase, the foot gets accelerated so that it can swing forward, and hence the frictional force now acts in the positive x direction, i.e. in the direction of walking. All this is reflected in the plot of GRF_x. The plot of GRF_y has a characteristic M-shape, which is typical of walking of healthy individuals. This M-shape curve results from the upward and downward acceleration of the CoM of the whole body during walking.

Thus, we have discussed how the kinematic/gait data is collected, how the different markers placed on the body correspond to the hip, knee and ankle locations, and how long does each phase of the gait cycle last for. We also looked at plots of the components of the ground reaction force, which were collected using force plates. In the next chapter, we will discuss different inverse dynamics models that can give us the required joint reactions and moments.

CHAPTER 3

INVERSE DYNAMICS ANALYSIS

3.1 2D analysis with GRF prescribed

An inverse dynamics analysis is necessary to estimate the joint reactions and moments. For the first type of analysis, we consider walking to be a two-dimensional (2D) activity, that is, the analysis is done in the sagittal plane only. We consider three bodies in the mechanism, which is the thigh/femur (between the hip and knee joint), the shank/tibia (between the knee and ankle joint), and the foot. The thigh and shank are assumed to be rods of a certain mass and length, and the foot is assumed to be like a triangle. We carry out the analysis for the right side only, as values of joint reactions/moments for the left side will simply be phase shifted. The hip and knee joints only allow flexion/extension, and the ankle joint only allows plantarflexion/dorsiflexion. Let the thigh be link 1, shank be link 2, and foot be link 3. This is illustrated in figure 3.1.

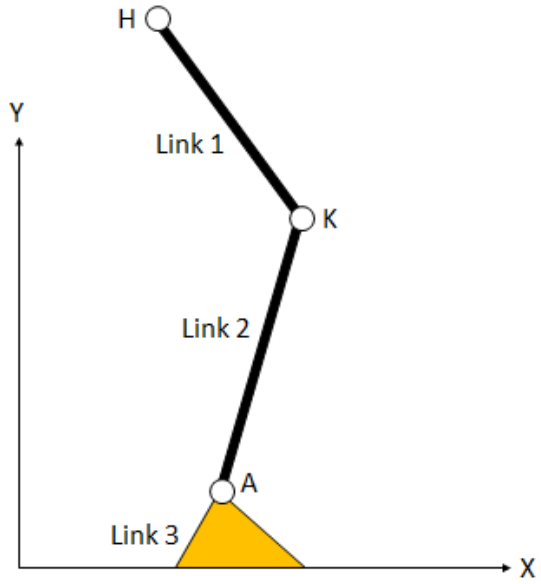

Figure 3.1: Model of the right leg

The x-axis is along the AP axis, and the y-axis is along the longitudinal axis. The system has 5 degrees of freedom (DOF), which are x_{hip}, y_{hip}, θ_1, θ_2 and θ_3. Here

x_{hip} is the x-coordinate, and y_{hip} is the y-coordinate of the hip. These DOF are depicted in figure 3.2.

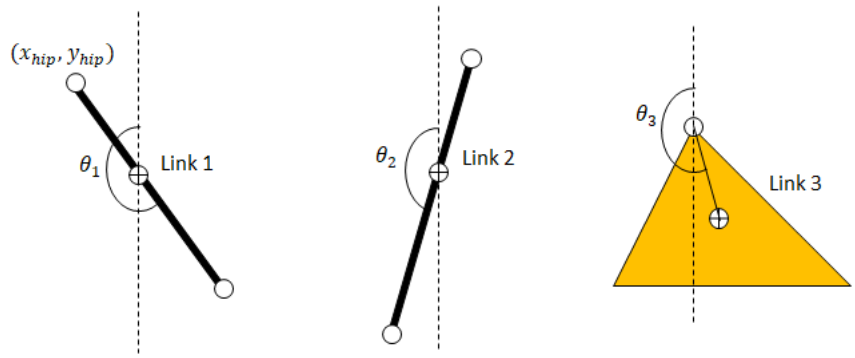

Figure 3.2: The 5 DOF of the system.

Let the length of the thigh and shank be L_1 and L_2 respectively. Let the CoM of the thigh, shank and foot be located at a distance of r_1, r_2 and r_3 from the hip, knee and ankle, respectively. Thus, we have

$$x_1 = x_{\text{hip}} - r_1 \sin\theta_1 \tag{3.1}$$

$$y_1 = y_{\text{hip}} + r_1 \cos\theta_1 \tag{3.2}$$

$$x_2 = x_{\text{hip}} - L_1 \sin\theta_1 - r_2 \sin\theta_2 \tag{3.3}$$

$$y_2 = y_{\text{hip}} + L_1 \cos\theta_1 + r_2 \cos\theta_2 \tag{3.4}$$

$$x_3 = x_{\text{hip}} - L_1 \sin\theta_1 - L_2 \sin\theta_2 - r_3 \sin\theta_3 \tag{3.5}$$

$$y_3 = y_{\text{hip}} + L_1 \cos\theta_1 + L_2 \cos\theta_2 + r_3 \cos\theta_3 \tag{3.6}$$

where (x_1, y_1), (x_2, y_2) and (x_3, y_3) are the coordinates of the CoM of the thigh, shank and foot respectively. Also, we can approximately say that

$$x_3 = \frac{x_{\text{ankle}} + x_{\text{heel}} + x_{\text{forefoot}}}{3} \tag{3.7}$$

$$y_3 = \frac{y_{\text{ankle}} + y_{\text{heel}} + y_{\text{forefoot}}}{3} \tag{3.8}$$

Now, we know the hip, knee, ankle, heel and forefoot coordinates from the gait data. Hence, they can be used to find the angles θ_1, θ_2 and θ_3. They are given by

$$\theta_1 = \frac{\pi}{2} + \text{atan2}(y_{\text{hip}} - y_{\text{knee}}, x_{\text{hip}} - x_{\text{knee}}) \tag{3.9}$$

$$\theta_2 = \frac{\pi}{2} + \text{atan2}(y_{\text{knee}} - y_{\text{ankle}}, x_{\text{knee}} - x_{\text{ankle}}) \tag{3.10}$$

$$\theta_3 = \frac{\pi}{2} + \text{atan2}(y_{\text{ankle}} - y_3, x_{\text{ankle}} - x_3) \tag{3.11}$$

where the atan2 function denotes a four quadrant version of the arctan function. It allows us to recover angles over the entire range of $[-\pi, \pi]$. Once the angles are determined, a Fourier series is fit through them. The plots of these angles are now shown in figures 3.3 to 3.5.

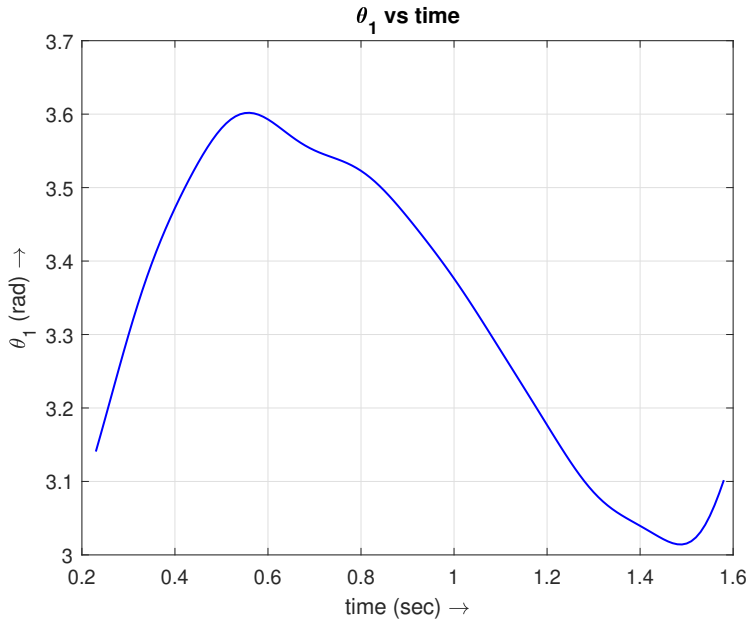

Figure 3.3: Variation of θ_1 versus time

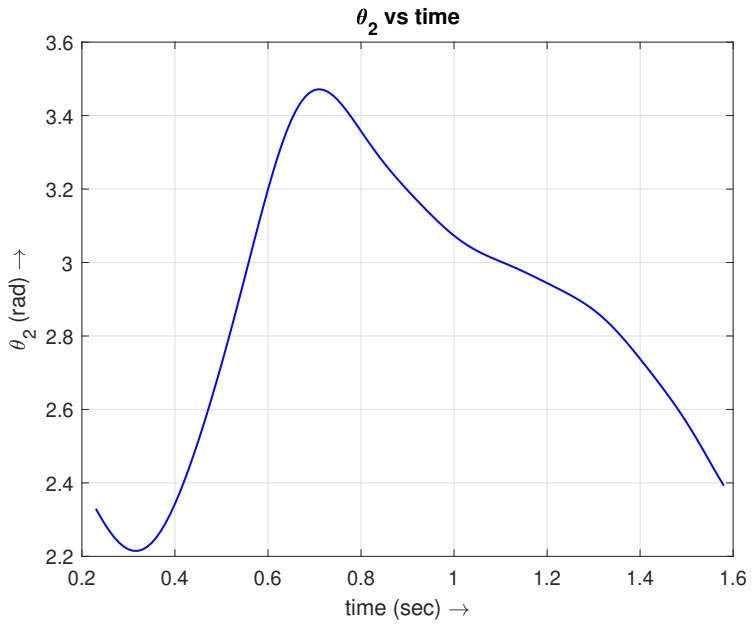

Figure 3.4: Variation of θ_2 versus time

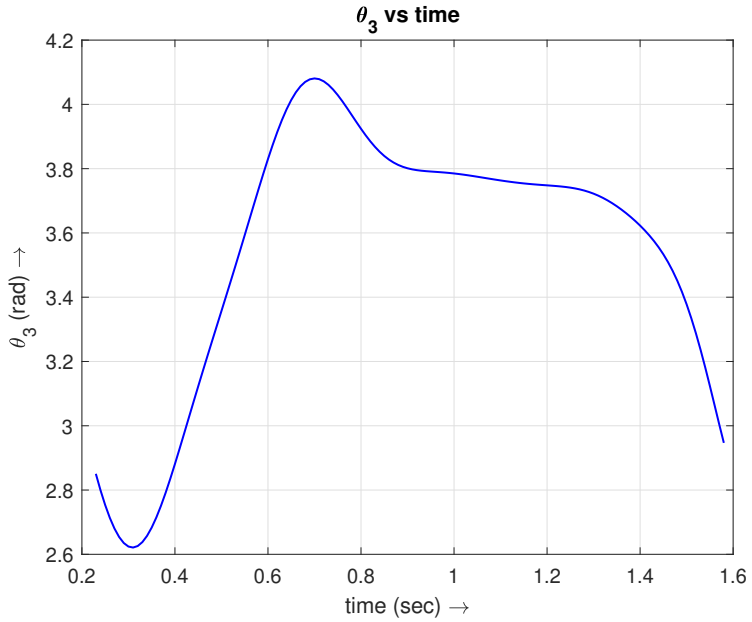

Figure 3.5: Variation of θ_3 versus time

We can now use Newton's method to determine the joint reactions and moments. The Free Body Diagrams (FBDs) of the links are shown in figure 3.6. The labelling convention is F_{ij} = force on link i from link j, and T_1, T_2 and T_3 are the torques at the hip, knee and ankle joint respectively, in the counterclockwise sense.

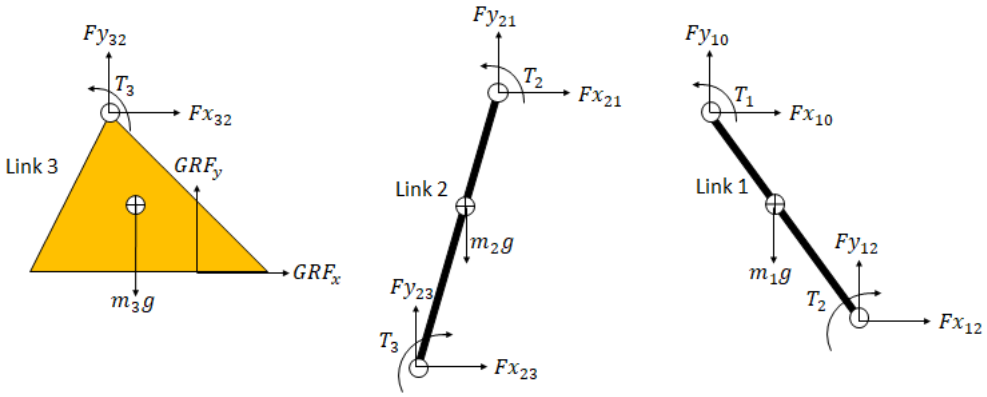

Figure 3.6: FBDs of the foot, shank and thigh

Let the mass of the thigh, shank and foot be m_1, m_2 and m_3 respectively. Similarly, let the moment of inertia of the thigh, shank and foot about their CoM be MI_1, MI_2 and MI_3 respectively. We now write the equations of motion of link 3, i.e. the foot, which are as follows

$$\text{GRF}_x + Fx_{32} = m_3\ddot{x}_3 \tag{3.12}$$

$$\mathrm{GRF}_y + Fy_{32} - m_3 g = m_3 \ddot{y}_3 \tag{3.13}$$

$$\begin{gathered}[r_3 \sin\theta_3, -r_3 \cos\theta_3] \otimes [Fx_{32}, Fy_{32}] + [x_{\mathrm{COP}} - x_3, y_{\mathrm{COP}} - y_3] \\ \otimes [\mathrm{GRF}_x, \mathrm{GRF}_y] + T_3 = \mathrm{MI}_3 \ddot{\theta}_3\end{gathered} \tag{3.14}$$

where $\otimes$ represents the 2D cross product, i.e. $[u_x, u_y] \otimes [v_x, v_y] = u_x v_y - u_y v_x$ for two vectors u and v. The COP here refers to the centre of pressure, which is the point on the surface of the foot where the ground reaction force acts. Its coordinates are also available from the force plate data. The only unknowns in these equations are Fx_{32}, Fy_{32} and T_3. Hence equations (3.12)-(3.14) can be solved for these three unknowns.

The equations of motion of link 2, i.e. the shank, are given by

$$Fx_{21} - Fx_{32} = m_2 \ddot{x}_2 \tag{3.15}$$

$$Fy_{21} - Fy_{32} - m_2 g = m_2 \ddot{y}_2 \tag{3.16}$$

$$\begin{gathered}[r_2 \sin\theta_2, -r_2 \cos\theta_2] \otimes [Fx_{21}, Fy_{21}] + [-(L_2 - r_2)\sin\theta_2, (L_2 - r_2)\cos\theta_2] \\ \otimes [-Fx_{32}, -Fy_{32}] + T_2 - T_3 = \mathrm{MI}_2 \ddot{\theta}_2\end{gathered} \tag{3.17}$$

where we have used the fact that $F_{ij} = -F_{ji}$, i.e. Newton's 3rd law. We have already calculated Fx_{32}, Fy_{32} and T_3 from equations (3.12)-(3.14). Thus, the only unknowns are Fx_{21}, Fy_{21} and T_2, which can be solved from equations (3.15)-(3.17).

Finally, the equations of motion of link 1, i.e. the thigh are given by

$$Fx_{10} - Fx_{21} = m_1 \ddot{x}_1 \tag{3.18}$$

$$Fy_{10} - Fy_{21} - m_1 g = m_1 \ddot{y}_1 \tag{3.19}$$

$$\begin{gathered}[r_1 \sin\theta_1, -r_1 \cos\theta_1] \otimes [Fx_{10}, Fy_{10}] + [-(L_1 - r_1)\sin\theta_1, (L_1 - r_1)\cos\theta_1] \\ \otimes [-Fx_{21}, -Fy_{21}] + T_1 - T_2 = \mathrm{MI}_1 \ddot{\theta}_1\end{gathered} \tag{3.20}$$

where F_{10} is the force acting on the hip due to the pelvis/trunk. We have already computed Fx_{21}, Fy_{21} and T_2 from equations (3.15)-(3.17). Hence, the only unknowns are Fx_{10}, Fy_{10} and T_1, which can be solved from equations (3.18)-(3.20). Therefore, we have calculated all the forces and moments at the hip, knee and ankle joint.

The equations (3.12)-(3.20) are symbolically evaluated in Mathematica, and expressions for the joint moments are obtained, which are then exported to MATLAB. The values of the masses, moment of inertias, length, and CoM locations of the thigh, shank and foot are taken from [5], and are given by

$$m_1 = 7.4 \text{ kg}, \; m_2 = 3.411 \text{ kg}, \; m_3 = 1.073 \text{ kg}$$

$$\text{MI}_1 = 0.1038 \text{ kg-m}^2, \; \text{MI}_2 = 0.05916 \text{ kg-m}^2, \; \text{MI}_3 = 0.01 \text{ kg-m}^2$$

$$L_1 = 0.4418 \text{ m}, \; L_2 = 0.4033 \text{ m}$$

$$r_1 = 0.1872 \text{ m}, \; r_2 = 0.1738 \text{ m}, \; r_3 = 0.044 \text{ m}$$

Using these values, and the expressions derived from Mathematica, the joint moments are computed, and their plots are now shown in figures 3.7 to 3.9.

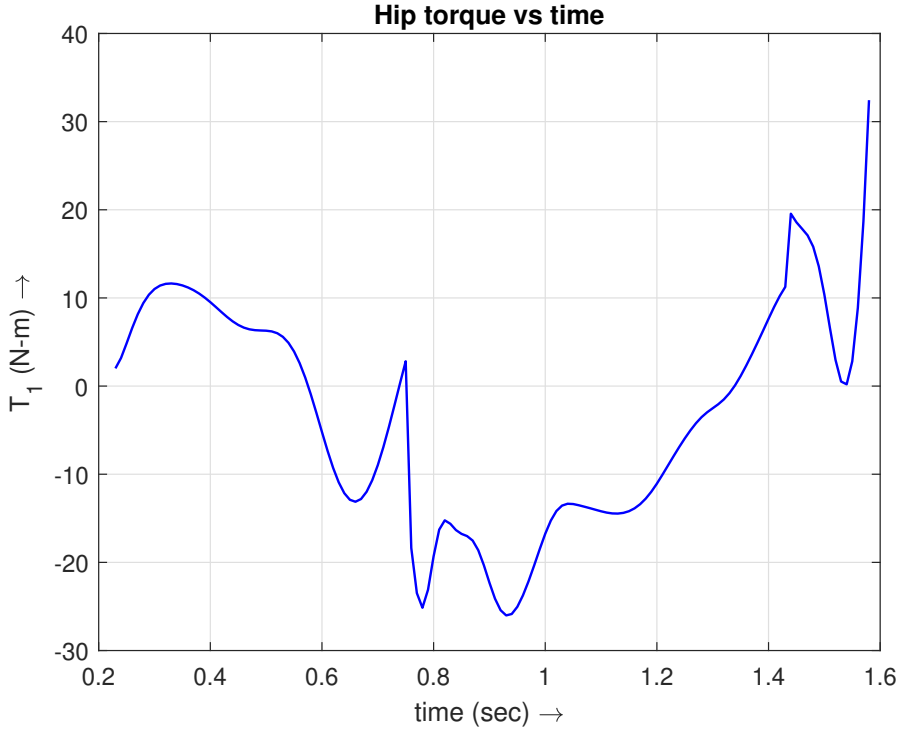

Figure 3.7: Variation of T_1 versus time

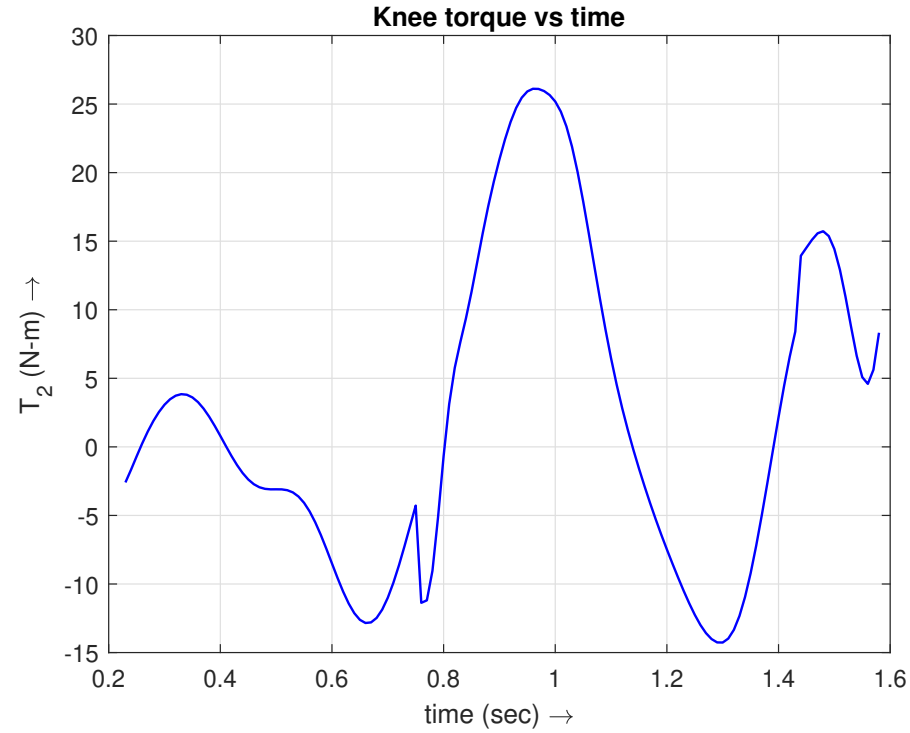

Figure 3.8: Variation of T_2 versus time

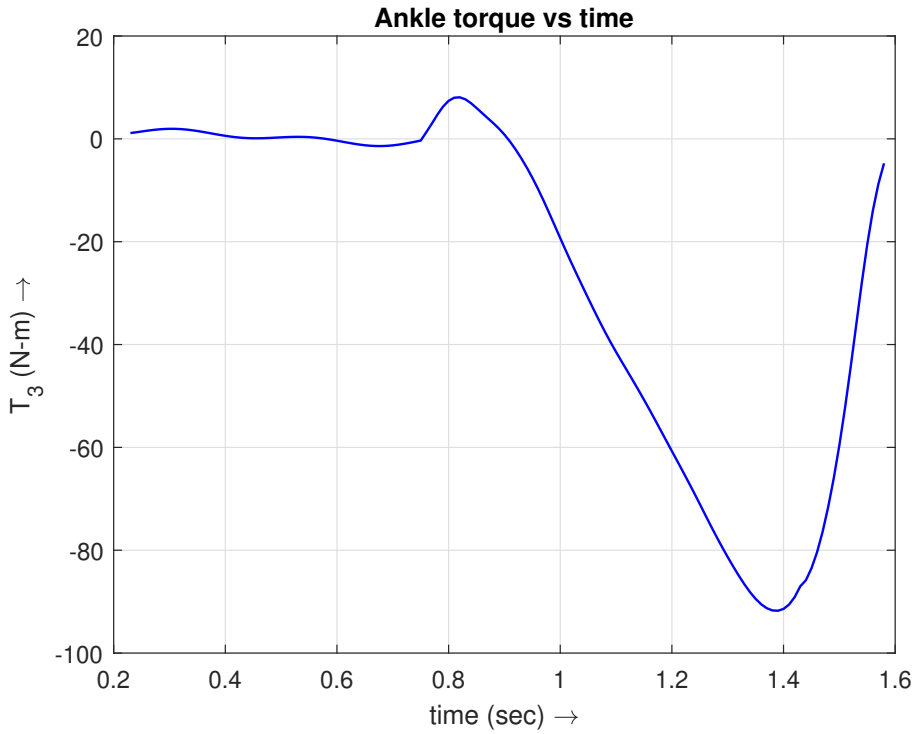

Figure 3.9: Variation of T_3 versus time

3.2 3D analysis with GRF prescribed - I

We now carry out a more complicated analysis in three dimensions (3D), to evaluate the joint moments and forces. The hip is modelled as a ball and socket joint, which has 3 DOF. It thus allows flexion/extension in the sagittal plane, abduction/adduction in the frontal plane, and internal/external rotation in the transverse plane. The knee is a simple hinge joint, which allows flexion/extension in the sagittal plane. We neglect the foot as of now in the analysis for simplicity, and include it later on (in section 3.3). We can further assume that the hip is brought to the coordinates (x_h, y_h, z_h) by three prismatic joints. Hence the system has 7 DOF. The thigh and shank are modelled as rods of a certain mass and length. We now use the Denavit-Hartenburg (DH) convention/algorithm to assign coordinate frames to the thigh and shank. There are many forms in which the DH convention is used. For this analysis, the algorithm is used in the following form (adapted from [4]):

Algorithm 1:

1. Number the joints from 1 to n starting with the base.
2. Assign a right-handed orthonormal coordinate frame L_0 to the base, making sure that Z^0 aligns with the axis of joint 1. Then set $i = 1$.
3. Align Z^i with the axis of joint $i + 1$.
4. Denote the origin of frame L_i by O_i. Locate O_i at the intersection of Z^i and Z^{i-1}. If they do not intersect, use the intersection of Z^i with a common normal between Z^i and Z^{i-1}.
5. Select X^i to be orthogonal to both Z^i and Z^{i-1}. If Z^i and Z^{i-1} are parallel, then align X^i in the direction of the common normal between Z^i and Z^{i-1}.
6. Select Y^i to form a right handed coordinate frame L_i.
7. Locate a point b_i at the intersection of X^i and Z^{i-1} axes. If they do not intersect, use the intersection of X^i with a common normal between X^i and Z^{i-1}.
8. Set $i = i + 1$. If $i \leq n$, go back to step 3. If $i > n$, exit the algorithm.

Algorithm 1 is applied to this mechanism, and is illustrated in figure 3.10.

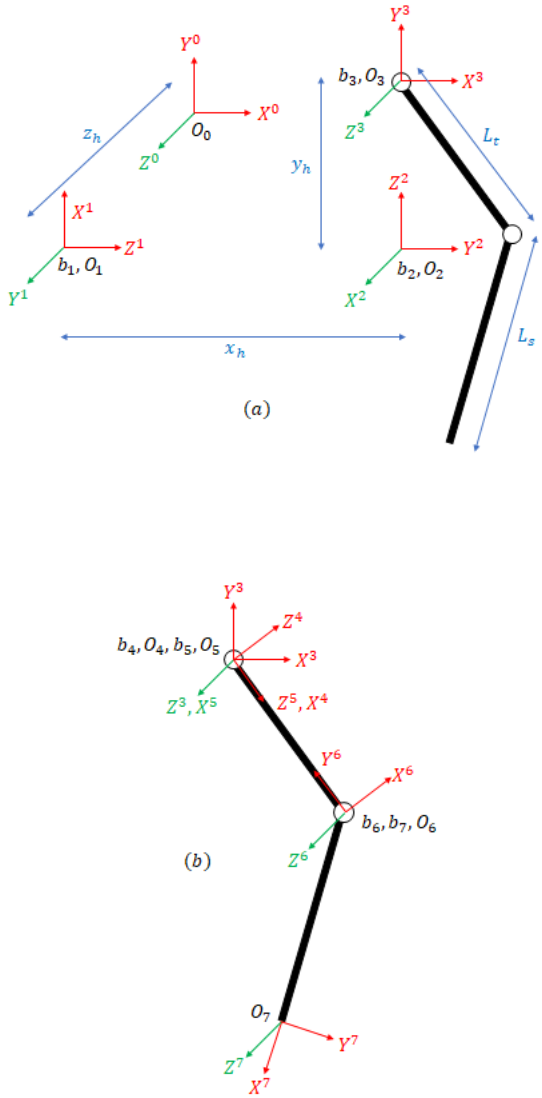

Figure 3.10: (a) Assignment of the first four frames and (b) assignment of the remaining frames, as per algorithm 1.

The X^0 axis is along the AP axis, the Y^0 axis is along the longitudinal axis and the Z^0 axis is along the ML axis. The 'red' axes represent the axes in the plane of the paper, and the 'green' axes represent the ones coming out of the plane of the paper. Note that the ball and socket joint at the hip is expressed by using three intersecting revolute joints. Once the coordinate frames have been assigned, the next step is to calculate the four DH parameters, which are the joint angle ϕ, joint distance d, link length a, and link twist angle β. They are computed as follows:

- Joint angle ϕ_i is the angle of rotation from X^{i-1} to X^i measured about Z^{i-1}.
- Joint distance d_i is the distance from O_{i-1} to point b_i measured along Z^{i-1}.
- Link length a_i is the distance from point b_i to O_i measured along X^i.

- Link twist angle β_i is the angle of rotation from Z^{i-1} to Z^i measured about X^i.

The link length and link twist angle are always constant for any joint. For a revolute joint, the joint angle is variable, but the joint distance is constant. Whereas for a prismatic joint, the joint distance is variable, but the joint angle is constant. The DH parameters for this mechanism are tabulated in table 3.1.

Table 3.1: DH parameters for the mechanism in figure 3.10

Axis	ϕ_i	d_i	a_i	β_i
$i=1$	$\pi/2$	z_h	0	$\pi/2$
$i=2$	$\pi/2$	x_h	0	$\pi/2$
$i=3$	$\pi/2$	y_h	0	$\pi/2$
$i=4$	θ_1	0	0	$-\pi/2$
$i=5$	θ_2	0	0	$-\pi/2$
$i=6$	θ_3	L_t	0	$-\pi/2$
$i=7$	θ_4	0	L_s	0

The angles θ_1, θ_2 and θ_3 characterize flexion/extension, abduction/adduction and internal/external rotation at the hip respectively. The angle θ_4 characterizes the flexion/extension at the knee. Also, L_t and L_s are the lengths of the thigh and shank respectively.

Now that the DH parameters have been computed, we can evaluate the link coordinate transformation matrix, which is given by

$$T_i^{i-1} = \begin{bmatrix} \cos\phi_i & -\cos\beta_i \sin\phi_i & \sin\beta_i \sin\phi_i & a_i \cos\phi_i \\ \sin\phi_i & \cos\beta_i \cos\phi_i & -\sin\beta_i \cos\phi_i & a_i \sin\phi_i \\ 0 & \sin\beta_i & \cos\beta_i & d_i \\ 0 & 0 & 0 & 1 \end{bmatrix} \tag{3.21}$$

where $i = 1, 2, \ldots, 7$. The next task is to perform an inverse kinematics analysis, i.e. estimating the angles θ_1, θ_2, θ_3 and θ_4. For this, we need to express the knee

and ankle (end of shank) coordinates in terms of these angles. We have

$$T_6^0 = T_1^0 T_2^1 T_3^2 T_4^3 T_5^4 T_6^5 \tag{3.22}$$

$$T_7^0 = T_6^0 T_7^6 \tag{3.23}$$

The first three elements of the last column of T_6^0 give us the knee coordinates, and similarly the first three elements of the last column of T_7^0 give us the ankle coordinates. Note that the hip, knee and ankle coordinates are available from gait data. The expressions of the knee coordinates from equation (3.22) are given by

$$x_k = x_h - L_t \sin\theta_2 \cos\theta_1 \tag{3.24}$$

$$y_k = y_h - L_t \sin\theta_1 \sin\theta_2 \tag{3.25}$$

$$z_k = z_h - L_t \cos\theta_2 \tag{3.26}$$

Thus we have

$$\begin{aligned} \cos\theta_2 &= \frac{z_h - z_k}{L_t} \\ \implies \theta_2 &= \arccos\left(\frac{z_h - z_k}{L_t}\right) \end{aligned} \tag{3.27}$$

Hence θ_2 can be evaluated. Now we have

$$\begin{aligned} \cos\theta_1 = c_1 &= \frac{x_h - x_k}{L_t \sin\theta_2} \\ \sin\theta_1 = s_1 &= \frac{y_h - y_k}{L_t \sin\theta_2} \\ \implies \theta_1 &= \text{atan2}(s_1, c_1) \end{aligned} \tag{3.28}$$

and so θ_1 can also be evaluated, since we now know θ_2 from equation (3.27). The ankle coordinates from equation (3.23) are given by

$$x_a = x_k + L_s\left(\sin\theta_1 \sin\theta_3 \cos\theta_4 + \cos\theta_1\left(\sin\theta_2 \sin\theta_4 + \cos\theta_2 \cos\theta_3 \cos\theta_4\right)\right) \tag{3.29}$$

$$y_a = y_k + L_s\left(\sin\theta_1 \sin\theta_2 \sin\theta_4 + \cos\theta_4\left(\sin\theta_1 \cos\theta_2 \cos\theta_3 - \sin\theta_3 \cos\theta_1\right)\right) \tag{3.30}$$

$$z_a = z_k + L_s\left(\sin\theta_4 \cos\theta_2 - \sin\theta_2 \cos\theta_3 \cos\theta_4\right) \tag{3.31}$$

We know all the coordinates from gait data, and angles θ_1 and θ_2 from equations

(3.27) and (3.28). Thus the above equations (3.29)-(3.31) comprise a linear system of three equations in three unknowns, which are: $\sin\theta_3\cos\theta_4$, $\cos\theta_3\cos\theta_4$ and $\sin\theta_4$. Solving the linear system (3.29)-(3.31), we get

$$\sin\theta_4 = s_4 = \frac{x_a\sin\theta_2\cos\theta_1 + y_a\sin\theta_1\sin\theta_2 + z_a\cos\theta_2 - x_k\sin\theta_2\cos\theta_1 - y_k\sin\theta_1\sin\theta_2 - z_k\cos\theta_2}{L_s}$$

$$\implies \theta_4 = \arcsin(s_4) \tag{3.32}$$

Hence, θ_4 is evaluated. Similarly, from the solution of the linear system (3.29)-(3.31), we also have

$$\sin\theta_3\cos\theta_4 = s_3c_4 = \frac{(y_k - y_a)\cos\theta_1 + x_a\sin\theta_1 - x_k\sin\theta_1}{L_s}$$

$$\cos\theta_3\cos\theta_4 = c_3c_4 = \frac{x_a\cos\theta_1\cos\theta_2 + y_a\sin\theta_1\cos\theta_2 - z_a\sin\theta_2 - x_k\cos\theta_1\cos\theta_2 - y_k\sin\theta_1\cos\theta_2 + z_k\sin\theta_2}{L_s}$$

$$\implies \theta_3 = \text{atan2}\left(\frac{s_3c_4}{\cos\theta_4}, \frac{c_3c_4}{\cos\theta_4}\right) \tag{3.33}$$

Thus θ_3 is also evaluated, since we know θ_4 from equation (3.32). Once all the angles are determined, a Fourier series is fit through each of them. The plots of these angles are now shown in figures 3.11 to 3.14.

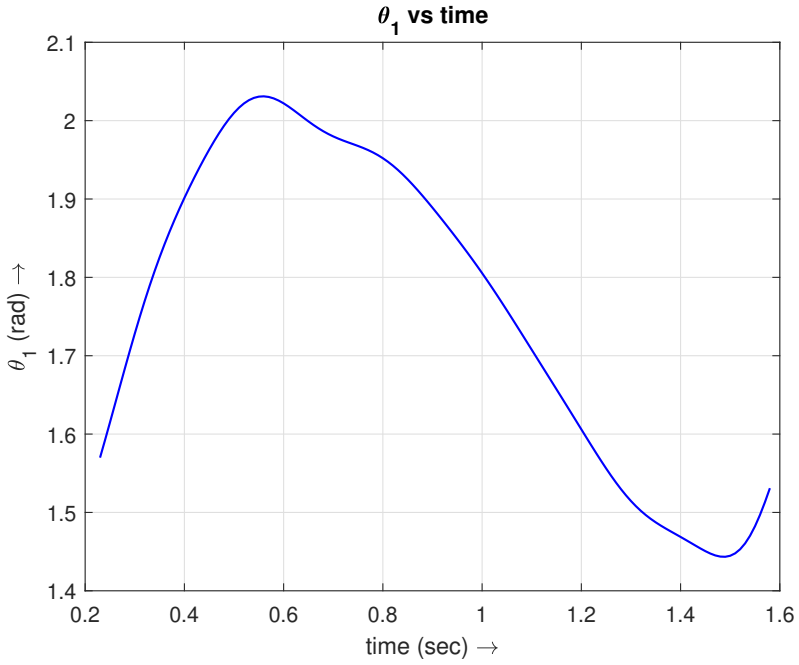

Figure 3.11: Variation of θ_1 versus time

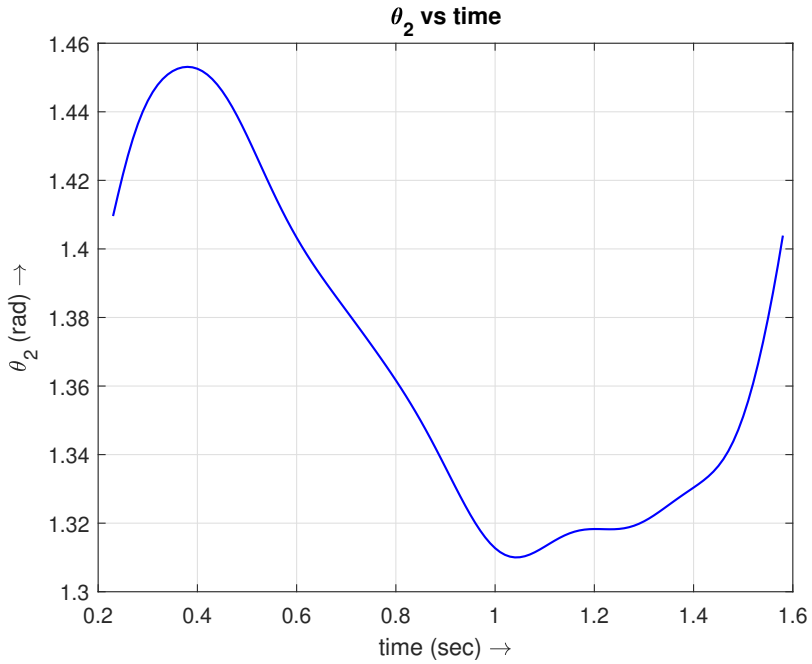

Figure 3.12: Variation of θ_2 versus time

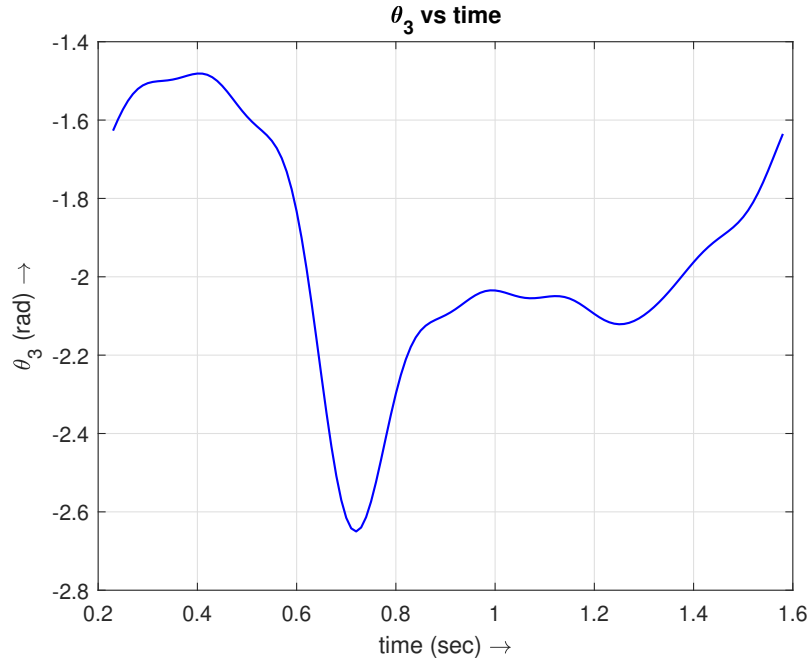

Figure 3.13: Variation of θ_3 versus time

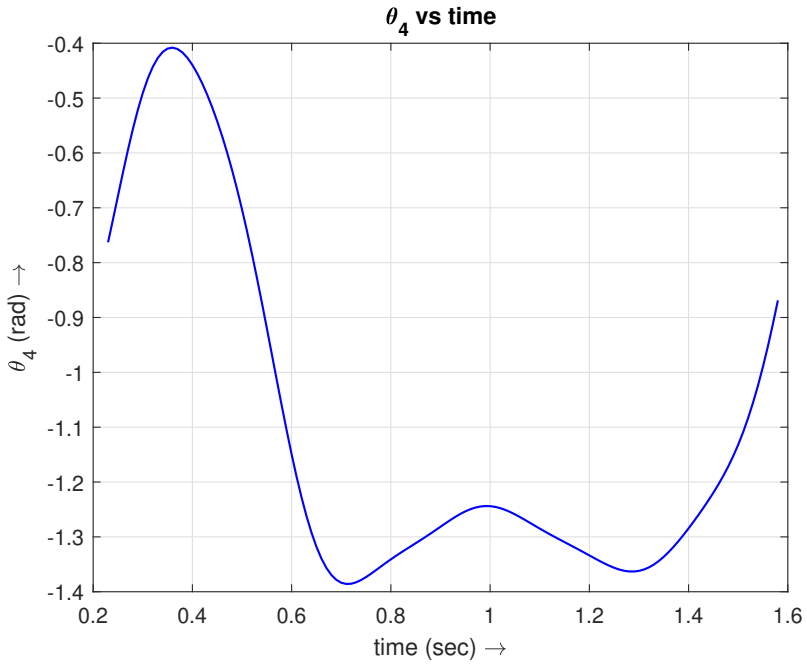

Figure 3.14: Variation of θ_4 versus time

We now use the Newton-Euler formulation to compute the joint reactions and moments. The first task is to find the link angular velocity, angular acceleration and linear acceleration. Let the set of joint variables be

$$q = [z_h \;\; x_h \;\; y_h \;\; \theta_1 \;\; \theta_2 \;\; \theta_3 \;\; \theta_4]^T \tag{3.34}$$

If joint i is prismatic, we have

$$\begin{aligned} & \omega_i^0 = \omega_{i-1}^0 \\ \implies & (R_0^i)\omega_i^0 = (R_0^i)\omega_{i-1}^0 \\ \implies & \omega_i = (R_{i-1}^i)(R_0^{i-1})\omega_{i-1}^0 = R_{i-1}^i \omega_{i-1} \end{aligned} \tag{3.35}$$

where ω_i^0 is the angular velocity of frame i (which is rigidly attached to link i) with respect to the base frame (frame 0), and ω_i denotes the angular velocity of frame i expressed in frame i. Similarly, we have

$$\begin{aligned} & \dot{\omega}_i^0 = \dot{\omega}_{i-1}^0 \\ \implies & (R_0^i)\dot{\omega}_i^0 = (R_0^i)\dot{\omega}_{i-1}^0 \\ \implies & \alpha_i = (R_{i-1}^i)(R_0^{i-1})\dot{\omega}_{i-1}^0 = R_{i-1}^i \alpha_{i-1} \end{aligned} \tag{3.36}$$

where α_i^0 is the angular acceleration of frame i with respect to the base frame, and α_i denotes the angular acceleration of frame i expressed in frame i
Now if joint i is a revolute joint, we have

$$\omega_i^0 = \omega_{i-1}^0 + \dot{q}_i z_{i-1}^0 \tag{3.37}$$

which represents the fact that the angular velocity of frame i equals that of frame $i-1$ plus the added rotation from joint i. Pre-multiplying both sides of equation (3.37) with R_0^i, we get

$$\begin{aligned} R_0^i\omega_i^0 &= R_0^i\omega_{i-1}^0 + \dot{q}_i R_0^i z_{i-1}^0 \\ \implies \omega_i &= (R_{i-1}^i)(R_0^{i-1})\omega_{i-1}^0 + \dot{q}_i(R_{i-1}^i)(R_0^{i-1})z_{i-1}^0 \\ \implies \omega_i &= R_{i-1}^i\omega_{i-1} + \dot{q}_i R_{i-1}^i z_{i-1} \end{aligned} \tag{3.38}$$

Since $z_{i-1} = [0\ \ 0\ \ 1]^T$, equation (3.38) becomes

$$\omega_i = R_{i-1}^i \left(\omega_{i-1} + \begin{bmatrix} 0 \\ 0 \\ \dot{q}_i \end{bmatrix} \right) \tag{3.39}$$

We have for the angular acceleration

$$\begin{aligned} \dot{\omega}_i^0 &= \dot{\omega}_{i-1}^0 + \ddot{q}_i z_{i-1}^0 + \omega_{i-1}^0 \times \dot{q}_i z_{i-1}^0 \\ \implies (R_0^i)\dot{\omega}_i^0 &= (R_0^i)\dot{\omega}_{i-1}^0 + \ddot{q}_i(R_0^i)z_{i-1}^0 + (R_0^i)\omega_{i-1}^0 \times \dot{q}_i(R_0^i)z_{i-1}^0 \\ \implies \alpha_i &= \\ (R_{i-1}^i)(R_0^{i-1})\dot{\omega}_{i-1}^0 &+ \ddot{q}_i(R_{i-1}^i)(R_0^{i-1})z_{i-1}^0 + (R_{i-1}^i)(R_0^{i-1})\omega_{i-1}^0 \times \dot{q}_i(R_{i-1}^i)(R_0^{i-1})z_{i-1}^0 \\ \implies \alpha_i &= R_{i-1}^i\alpha_{i-1} + \ddot{q}_i R_{i-1}^i z_{i-1} + R_{i-1}^i\omega_{i-1} \times \dot{q}_i R_{i-1}^i z_{i-1} \\ \implies \alpha_i &= R_{i-1}^i\left(\alpha_{i-1} + \ddot{q}_i z_{i-1} + \omega_{i-1} \times \dot{q}_i z_{i-1}\right) \\ \implies \alpha_i &= R_{i-1}^i \left(\alpha_{i-1} + \omega_{i-1} \times \begin{bmatrix} 0 \\ 0 \\ \dot{q}_i \end{bmatrix} + \begin{bmatrix} 0 \\ 0 \\ \ddot{q}_i \end{bmatrix} \right) \end{aligned} \tag{3.40}$$

Thus we can evaluate the angular velocity and angular acceleration of each frame i. We now compute the linear acceleration of each link. If joint i is revolute, we

have

$$
\begin{aligned}
a_i^0 &= a_{i-1}^0 + \alpha_i^0 \times \Delta s_i^0 + \omega_i^0 \times \left(\omega_i^0 \times \Delta s_i^0\right) \\
\implies (R_0^i)a_i^0 &= (R_0^i)a_{i-1}^0 + (R_0^i)\alpha_i^0 \times (R_0^i)\Delta s_i^0 + (R_0^i)\omega_i^0 \times \left((R_0^i)\omega_i^0 \times (R_0^i)\Delta s_i^0\right) \\
\implies a_i &= R_{i-1}^i a_{i-1} + \alpha_i \times (R_0^i)\Delta s_i^0 + \omega_i \times \left(\omega_i \times (R_0^i)\Delta s_i^0\right) \qquad (3.41)
\end{aligned}
$$

where a_i^0 is the acceleration of the origin of frame i expressed in the base frame, and a_i is the acceleration of the origin of frame i expressed in frame i, and further

$$\Delta s_i^0 = p_i^0 - p_{i-1}^0 \qquad (3.42)$$

where p_i^0 is the position of the origin of frame i with respect to the base frame. Pre-multiplying both sides of equation (3.42) with R_0^i, we get

$$
\begin{aligned}
(R_0^i)\Delta s_i^0 &= (R_0^i)p_i^0 - (R_0^i)p_{i-1}^0 \\
\implies (R_0^i)\Delta s_i^0 &= p_i^i - p_{i-1}^i = -p_{i-1}^i \qquad (3.43)
\end{aligned}
$$

since $p_i^i = [0\ \ 0\ \ 0]^T$. Let $r_{i,i+1}$ be the vector from the origin of frame $i-1$ to the origin of frame i, expressed in frame i, or alternatively it is the vector from joint i to joint $i+1$, expressed in frame i. Thus we have

$$
\begin{aligned}
p_{i-1}^i &= -r_{i,i+1} \\
\implies (R_0^i)\Delta s_i^0 &= -p_{i-1}^i = r_{i,i+1} \qquad (3.44)
\end{aligned}
$$

Hence the expression for a_i (equation (3.41)) becomes

$$a_i = R_{i-1}^i a_{i-1} + \alpha_i \times r_{i,i+1} + \omega_i \times (\omega_i \times r_{i,i+1}) \qquad (3.45)$$

Since frame i is rigidly attached to the end of link i, we can rather denote a_i as $a_{e,i}$. Similarly, the expression for the acceleration of the CoM of link i with respect to frame i is given by

$$a_{c,i} = R_{i-1}^i a_{e,i-1} + \alpha_i \times r_{i,ci} + \omega_i \times (\omega_i \times r_{i,ci}) \qquad (3.46)$$

where $r_{i,ci}$ is the vector from joint i to the CoM of link i, expressed in frame i.

Now if joint i is prismatic, we have

$$\begin{aligned}
& a^0_{e,i} = a^0_{e,i-1} + \alpha^0_i \times \Delta s^0_i + \omega^0_i \times \left(\omega^0_i \times \Delta s^0_i\right) + \ddot{q}_i z^0_{i-1} + 2\omega^0_i \times \dot{q}_i z^0_{i-1} \\
\implies & (R^i_0)a^0_{e,i} = (R^i_0)a^0_{e,i-1} + (R^i_0)\alpha^0_i \times (R^i_0)\Delta s^0_i + (R^i_0)\omega^0_i \times \left((R^i_0)\omega^0_i \times (R^i_0)\Delta s^0_i\right) + \\
& \qquad \ddot{q}_i (R^i_0) z^0_{i-1} + 2(R^i_0)\omega^0_i \times \dot{q}_i (R^i_0) z^0_{i-1} \\
\implies & a_{e,i} = R^i_{i-1} a_{e,i-1} + \alpha_i \times r_{i,i+1} + \omega_i \times (\omega_i \times r_{i,i+1}) + \ddot{q}_i R^i_{i-1} z_{i-1} + 2\omega_i \times \dot{q}_i R^i_{i-1} z_{i-1} \\
\implies & a_{e,i} = R^i_{i-1} \left(a_{e,i-1} + 2\omega_i \times \begin{bmatrix} 0 \\ 0 \\ \dot{q}_i \end{bmatrix} + \begin{bmatrix} 0 \\ 0 \\ \ddot{q}_i \end{bmatrix} \right) + \alpha_i \times r_{i,i+1} + \omega_i \times (\omega_i \times r_{i,i+1})
\end{aligned} \tag{3.47}$$

Similarly we can write

$$a_{c,i} = R^i_{i-1} \left(a_{e,i-1} + 2\omega_i \times \begin{bmatrix} 0 \\ 0 \\ \dot{q}_i \end{bmatrix} + \begin{bmatrix} 0 \\ 0 \\ \ddot{q}_i \end{bmatrix} \right) + \alpha_i \times r_{i,ci} + \omega_i \times (\omega_i \times r_{i,ci}) \tag{3.48}$$

Thus the linear acceleration of each frame/link can be evaluated as well.
Note that joints 1, 2 and 3 are prismatic, whereas joints 4, 5, 6 and 7 are revolute. Also note that for the mechanism, the number of links/joints is $n = 7$. Hence, the link velocities and accelerations can be computed by the following algorithm:

Algorithm 2:

1. Start with the initial conditions

   $$\omega_0 = 0, \alpha_0 = 0, a_{e,0} = 0, a_{c,0} = 0$$

   and set $i = 1$.

2. Compute

   $$\begin{aligned}
   \omega_i &= R^i_{i-1}\omega_{i-1} \\
   \alpha_i &= R^i_{i-1}\alpha_{i-1} \\
   a_{e,i} &= R^i_{i-1} \left(a_{e,i-1} + 2\omega_i \times \begin{bmatrix} 0 \\ 0 \\ \dot{q}_i \end{bmatrix} + \begin{bmatrix} 0 \\ 0 \\ \ddot{q}_i \end{bmatrix} \right) + \alpha_i \times r_{i,i+1} + \omega_i \times (\omega_i \times r_{i,i+1}) \\
   a_{c,i} &= R^i_{i-1} \left(a_{e,i-1} + 2\omega_i \times \begin{bmatrix} 0 \\ 0 \\ \dot{q}_i \end{bmatrix} + \begin{bmatrix} 0 \\ 0 \\ \ddot{q}_i \end{bmatrix} \right) + \alpha_i \times r_{i,ci} + \omega_i \times (\omega_i \times r_{i,ci})
   \end{aligned}$$

3. Set $i = i + 1$. If $i \leq 3$, go back to step 2. If $i > 3$, go to step 4.

4. Compute

$$\omega_i = R_{i-1}^i \left(\omega_{i-1} + \begin{bmatrix} 0 \\ 0 \\ \dot{q}_i \end{bmatrix} \right)$$

$$\alpha_i = R_{i-1}^i \left(\alpha_{i-1} + \omega_{i-1} \times \begin{bmatrix} 0 \\ 0 \\ \dot{q}_i \end{bmatrix} + \begin{bmatrix} 0 \\ 0 \\ \ddot{q}_i \end{bmatrix} \right)$$

$$a_{e,i} = R_{i-1}^i a_{e,i-1} + \alpha_i \times r_{i,i+1} + \omega_i \times (\omega_i \times r_{i,i+1})$$

$$a_{c,i} = R_{i-1}^i a_{e,i-1} + \alpha_i \times r_{i,ci} + \omega_i \times (\omega_i \times r_{i,ci})$$

5. Set $i = i + 1$. If $i \leq n$, go back to step 4. If $i > n$, exit the algorithm.

Hence from this algorithm, the link angular velocity, angular acceleration and linear acceleration can be determined. The next and final step is to calculate the joint moment and forces. Consider the free body diagram of an arbitrary link i as shown in figure 3.15.

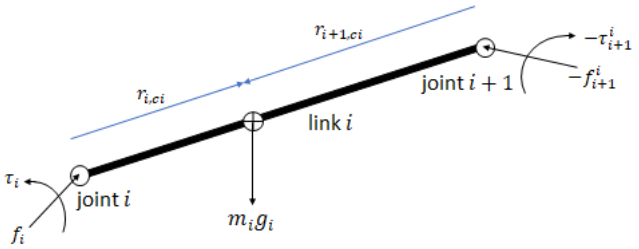

Figure 3.15: FBD of link i

Here, f_i is the force exerted by link $i-1$ on link i, τ_i is the torque exerted by link $i-1$ on link i, g_i is the acceleration due to gravity, and $r_{i+1,ci}$ is the vector from joint $i+1$ to the CoM of link i. All these vectors are expressed in frame i.
The force balance equation for link i is

$$\begin{aligned} & f_i - f_{i+1}^i + m_i g_i = m_i a_{c,i} \\ \implies & f_i - R_{i+1}^i f_{i+1} + m_i g_i = m_i a_{c,i} \\ \implies & f_i - R_{i+1}^i f_{i+1} + m_i R_0^i G = m_i a_{c,i} \\ \implies & f_i = R_{i+1}^i f_{i+1} + m_i a_{c,i} - m_i R_0^i G \end{aligned} \tag{3.49}$$

where m_i is the mass of link i, and $G = [0 \quad -g \quad 0]^T$.

Similarly, the moment equation for link i about its CoM is given by

$$\begin{aligned}
\tau_i - \tau_{i+1}^i + (-r_{i,ci}) \times f_i + (-r_{i+1,ci}) \times (-f_{i+1}^i) &= \mathrm{MI}_i \alpha_i + \omega_i \times (\mathrm{MI}_i \omega_i) \\
\implies \tau_i - \tau_{i+1}^i - r_{i,ci} \times f_i + r_{i+1,ci} \times f_{i+1}^i &= \mathrm{MI}_i \alpha_i + \omega_i \times (\mathrm{MI}_i \omega_i) \\
\implies \tau_i - R_{i+1}^i \tau_{i+1} - r_{i,ci} \times f_i + r_{i+1,ci} \times R_{i+1}^i f_{i+1} &= \mathrm{MI}_i \alpha_i + \omega_i \times (\mathrm{MI}_i \omega_i) \\
\implies \tau_i = R_{i+1}^i \tau_{i+1} + r_{i,ci} \times f_i - r_{i+1,ci} \times R_{i+1}^i f_{i+1} &+ \mathrm{MI}_i \alpha_i + \omega_i \times (\mathrm{MI}_i \omega_i)
\end{aligned} \tag{3.50}$$

where MI_i is the moment of inertia matrix of link i about a frame parallel to frame i and whose origin is at the CoM of link i. Note that the thigh and shank are link 6 and link 7 of the mechanism, respectively. All other links have essentially zero length, zero mass and zero moment of inertia. Let us denote the mass of the thigh and shank by m_t and m_s respectively. That is, $m_6 = m_t$ and $m_7 = m_s$. Similarly, $\mathrm{MI}_6 = \mathrm{MI}_t$ and $\mathrm{MI}_7 = \mathrm{MI}_s$. Also, since the axis of joint i coincides with Z^{i-1}, the torque at joint i is given by the third component of τ_i^{i-1}. That is

$$T_i = [0 \;\; 0 \;\; 1] \cdot \tau_i^{i-1} = [0 \;\; 0 \;\; 1] \cdot R_i^{i-1} \tau_i \tag{3.51}$$

where $\cdot$ denotes the vector dot product. More details about the Newton-Euler formulation can be found in [1] and [6].

The force balance and moment balance equations are written successively starting from $i = 7$, and we go all the way till $i = 1$. For our purpose it suffices to go till $i = 4$. Thus the following algorithm is used to compute the forces and moments.

Algorithm 3:

1. Start with the initial conditions

   $$f_{n+1} = \mathrm{GRF} = \begin{bmatrix} \mathrm{GRF}_x & \mathrm{GRF}_y & \mathrm{GRF}_z \end{bmatrix}^T, \tau_{n+1} = 0$$

   and set $i = n$.

2. Compute f_i, τ_i and T_i by

   $$\begin{aligned}
   f_i &= R_{i+1}^i f_{i+1} + m_i a_{c,i} - m_i R_0^i G \\
   \tau_i &= R_{i+1}^i \tau_{i+1} + r_{i,ci} \times f_i - r_{i+1,ci} \times R_{i+1}^i f_{i+1} + \mathrm{MI}_i \alpha_i + \omega_i \times (\mathrm{MI}_i \omega_i) \\
   T_i &= [0 \;\; 0 \;\; 1] \cdot R_i^{i-1} \tau_i
   \end{aligned}$$

   Also, set $R_{n+1}^n = R_0^n$, wherever it occurs.

3. Set $i = i - 1$. If $i \geq 4$, go back to step 2. If $i < 4$, exit the algorithm.

For more clarity, the force balance equations are shown below.

$$f_7 = R_0^7 \mathrm{GRF} + m_s a_{c,7} - m_s R_0^7 G \tag{3.52}$$

$$f_6 = R_7^6 f_7 + m_t a_{c,6} - m_t R_0^6 G \tag{3.53}$$

$$f_5 = R_6^5 f_6 \tag{3.54}$$

$$f_4 = R_5^4 f_5 \tag{3.55}$$

Similarly, the moment balance equations are

$$\tau_7 = r_{7,c7} \times f_7 - r_{8,c7} \times R_0^7 \mathrm{GRF} + \mathrm{MI}_s \alpha_7 + \omega_7 \times (\mathrm{MI}_s \omega_7) \tag{3.56}$$

$$\tau_6 = R_7^6 \tau_7 + r_{6,c6} \times f_6 - r_{7,c6} \times R_7^6 f_7 + \mathrm{MI}_t \alpha_6 + \omega_6 \times (\mathrm{MI}_t \omega_6) \tag{3.57}$$

$$\tau_5 = R_6^5 \tau_6 + r_{5,c5} \times f_5 - r_{6,c5} \times R_6^5 f_6 \tag{3.58}$$

$$\tau_4 = R_5^4 \tau_5 + r_{4,c4} \times f_4 - r_{5,c4} \times R_5^4 f_5 \tag{3.59}$$

From this, the joint torque T_i can then be computed from equation (3.51), or from algorithm 3.

The various vectors that are used in the above equations are given by

$$r_{4,5} = r_{5,6} = [0 \;\; 0 \;\; 0]^T$$

$$r_{6,7} = [0 \;\; -L_t \;\; 0]^T$$

$$r_{7,8} = [L_s \;\; 0 \;\; 0]^T$$

$$r_{4,c4} = r_{5,c5} = [0 \;\; 0 \;\; 0]^T$$

$$r_{6,c6} = [0 \;\; -r_t \;\; 0]^T$$

$$r_{7,c7} = [r_s \;\; 0 \;\; 0]^T$$

$$r_{5,c4} = r_{6,c5} = [0 \;\; 0 \;\; 0]^T$$

$$r_{7,c6} = [0 \;\; L_t - r_t \;\; 0]^T$$

$$r_{8,c7} = [-L_s + r_s \;\; 0 \;\; 0]^T$$

where r_t and r_s are the distances of the CoM of the thigh and shank from the hip and knee, respectively. All equations are symbolically evaluated in Mathematica (using algorithms 2 and 3), and expressions for the joint moments are obtained, which are then exported to MATLAB. The values of the masses, moment of inertia

matrices, lengths, and CoM locations are

$$m_t = 7.4 \text{ kg}, \; m_s = 3.411 \text{ kg}$$

$$L_t = 0.4418 \text{ m}, \; L_s = 0.4033 \text{ m}$$

$$r_t = 0.1872 \text{ m}, \; r_s = 0.1738 \text{ m}$$

$$\text{MI}_t = \begin{bmatrix} 0.1038 & 0 & 0 \\ 0 & 0 & 0 \\ 0 & 0 & 0.1038 \end{bmatrix} \text{ kg-m}^2$$

$$\text{MI}_s = \begin{bmatrix} 0 & 0 & 0 \\ 0 & 0.05916 & 0 \\ 0 & 0 & 0.05916 \end{bmatrix} \text{ kg-m}^2$$

Using these values, and the expressions derived from Mathematica, the joint moments are computed, and their plots are now shown in figures 3.16 to 3.19.

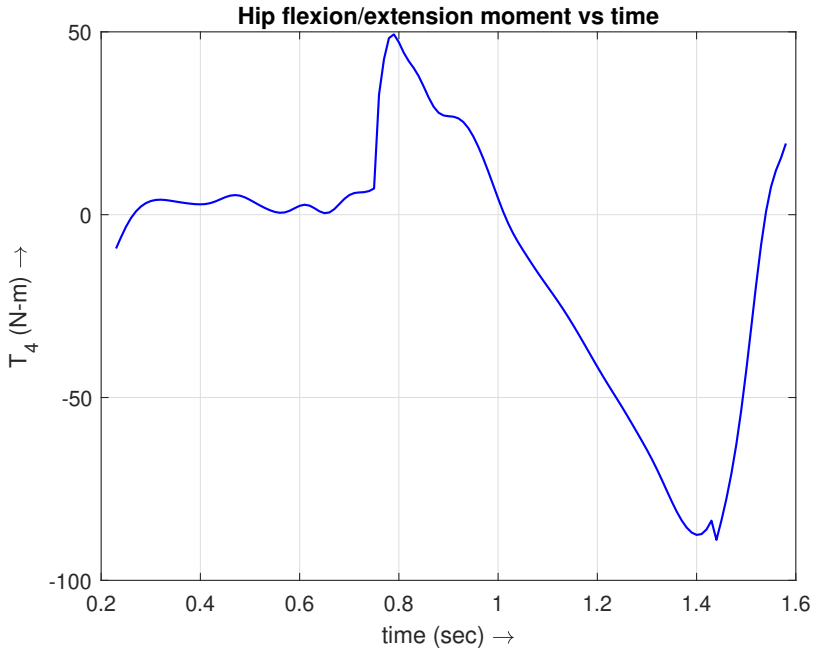

Figure 3.16: Variation of T_4 versus time

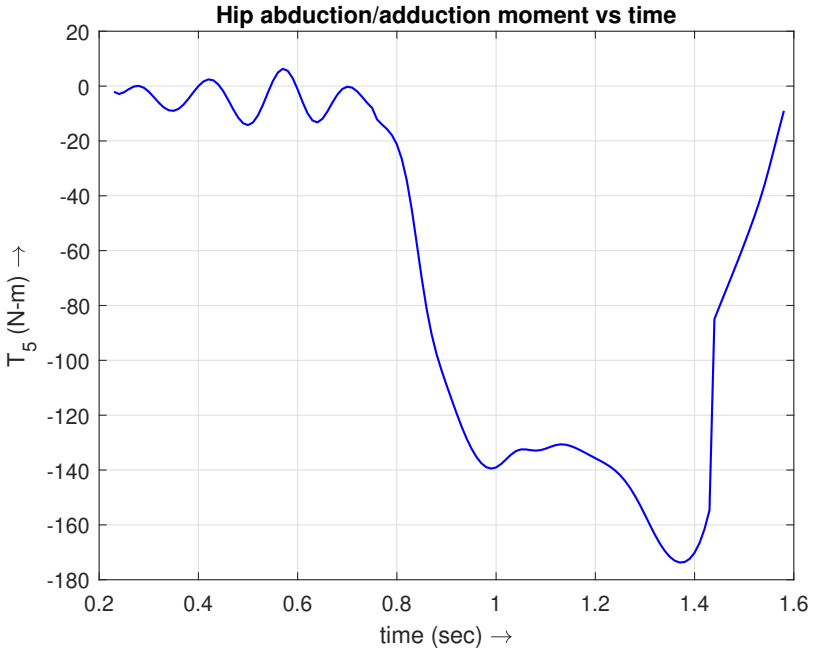

Figure 3.17: Variation of T_5 versus time

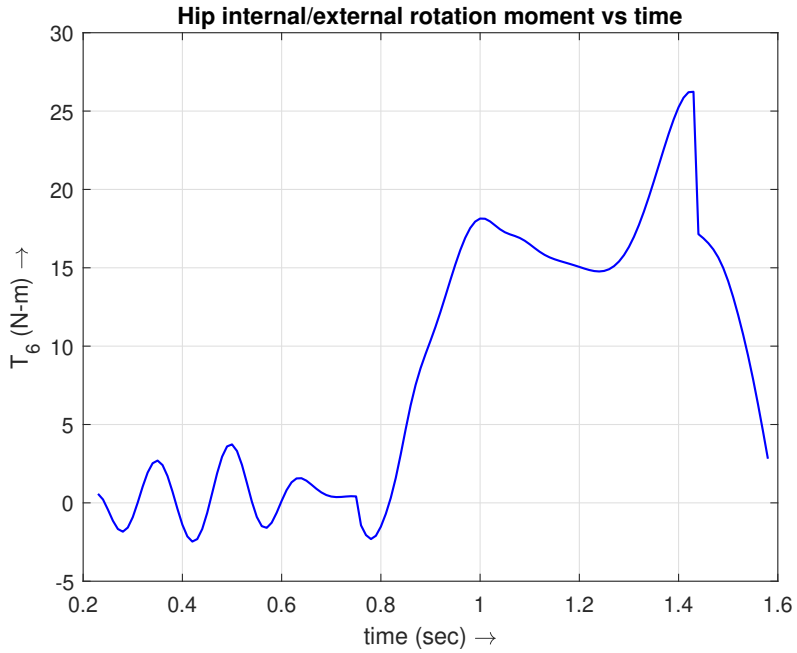

Figure 3.18: Variation of T_6 versus time

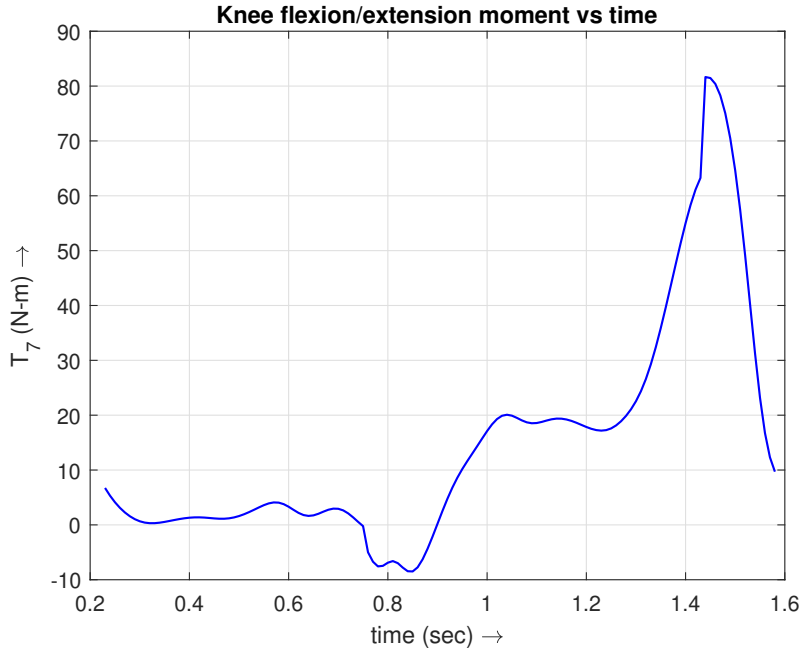

Figure 3.19: Variation of T_7 versus time

3.3 3D analysis with GRF prescribed - II

We now include the foot in the analysis, and it is modelled as a thin rod, just like the thigh and shank. To facilitate this, we make an approximation. We assume that coordinates of the ankle joint coincide with the heel, and so the foot is a rod of a certain mass and length, from the heel to the forefoot. The ankle joint is modelled as a 2 DOF joint that enables dorsiflexion/plantarflexion in the sagittal plane, and inversion/eversion in the frontal plane. We use algorithm 1 to assign coordinate frames to the mechanism. This is depicted in figure 3.20.

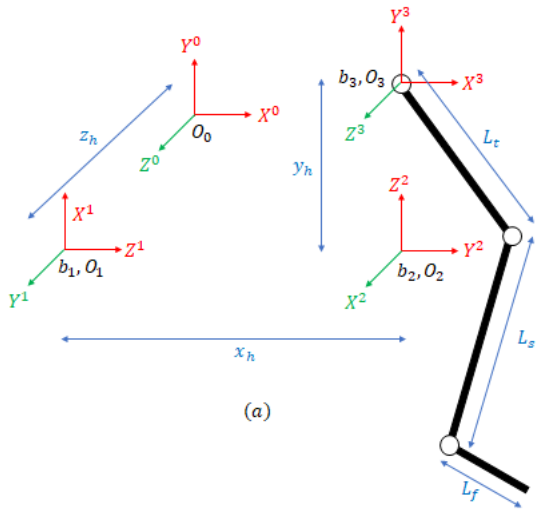

(a)

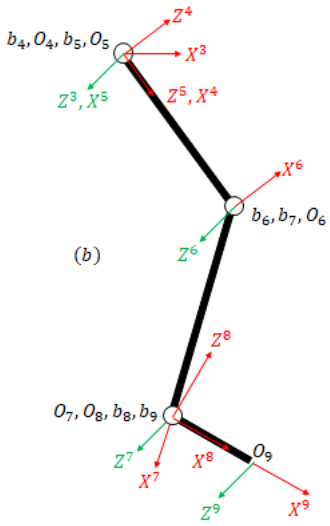

Figure 3.20: (a) Assignment of the first four frames and (b) assignment of the remaining frames, as per algorithm 1.

The y-axes have been omitted from the second figure for clarity. The D-H parameters for this mechanism are computed and are given in table 3.2.

Table 3.2: DH parameters for the mechanism in figure 3.20

Axis	ϕ_i	d_i	a_i	β_i
$i = 1$	$\pi/2$	z_h	0	$\pi/2$
$i = 2$	$\pi/2$	x_h	0	$\pi/2$
$i = 3$	$\pi/2$	y_h	0	$\pi/2$
$i = 4$	θ_1	0	0	$-\pi/2$
$i = 5$	θ_2	0	0	$-\pi/2$
$i = 6$	θ_3	L_t	0	$-\pi/2$
$i = 7$	θ_4	0	L_s	0
$i = 8$	θ_5	0	0	$-\pi/2$
$i = 9$	θ_6	0	L_f	$\pi/2$

Dorsiflexion/plantarflexion and inversion/eversion at the ankle are characterized by angles θ_5 and θ_6 respectively. Also, L_f denotes length of the foot.

The transformation matrices can now be computed (section 3.2, equation (3.21)), and the angles θ_1, θ_2, θ_3, and θ_4 are determined as before (section 3.2, equations

(3.27), (3.28), (3.32) and (3.33)). We now have to determine angles θ_5 and θ_6. We have

$$T_9^0 = T_7^0 T_8^7 T_9^8 \tag{3.60}$$

The first three elements of the last column of T_9^0 give us the coordinates of the forefoot. Let us denote them by (x_f, y_f, z_f). This time, we again get a linear system of three equations in three unknowns, the unknowns being: $\sin\theta_5 \cos\theta_6 (= s_5 c_6)$, $\cos\theta_5 \cos\theta_6 (= c_5 c_6)$ and $\sin\theta_6 (= s_6)$. We can solve this linear system to get the values of these unknowns, but their expressions have been omitted for sake of brevity. Essentially, we can get θ_5 and θ_6 by

$$\theta_6 = \arcsin s_6 \tag{3.61}$$

$$\theta_5 = \text{atan2}\left(\frac{s_5 c_6}{\cos\theta_6}, \frac{c_5 c_6}{\cos\theta_6}\right) \tag{3.62}$$

Their plots are now shown in figures 3.21 and 3.22.

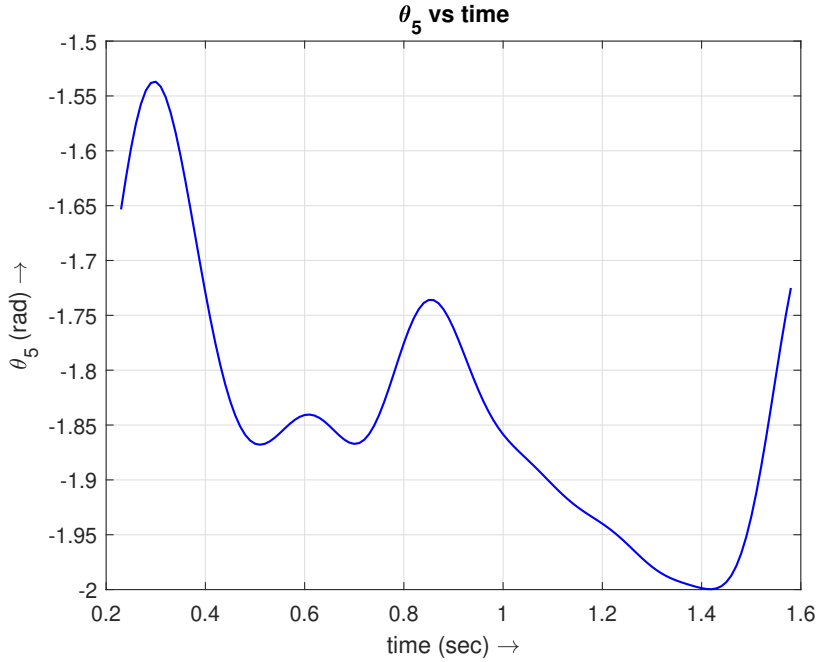

Figure 3.21: Variation of θ_5 versus time

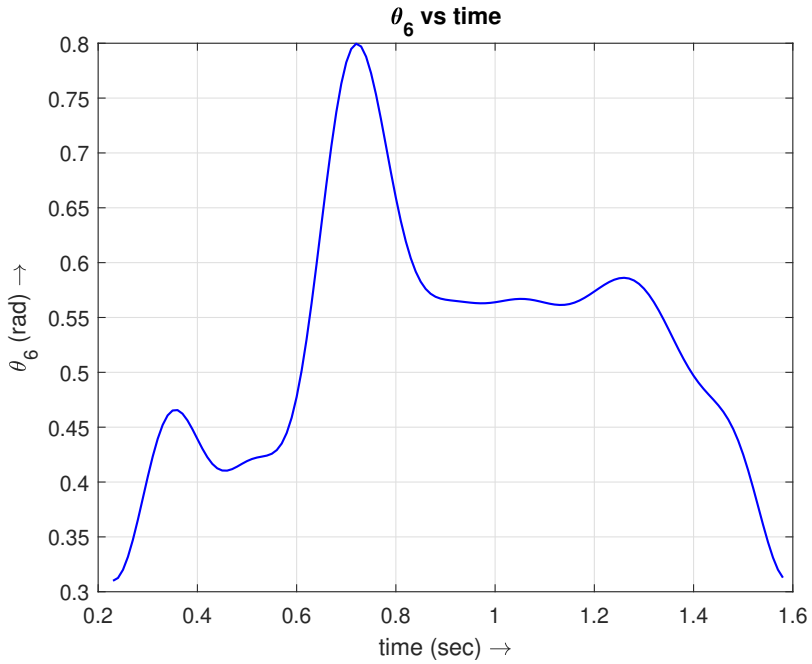

Figure 3.22: Variation of θ_6 versus time

We now use algorithm 2 and algorithm 3 with $n = 9$ to calculate the link velocities and accelerations, followed by the joint forces and moments. The foot here is link 9 of the mechanism. The system has 9 DOF, and the joint variables are given by

$$q = [z_h \;\; x_h \;\; y_h \;\; \theta_1 \;\; \theta_2 \;\; \theta_3 \;\; \theta_4 \;\; \theta_5 \;\; \theta_6]^T \tag{3.63}$$

The additional vectors to be used in the algorithms due to the addition of the foot in the mechanism are given by

$$r_{8,9} = [0 \;\; 0 \;\; 0]^T$$
$$r_{9,10} = [L_f \;\; 0 \;\; 0]^T$$
$$r_{8,c8} = [0 \;\; 0 \;\; 0]^T$$
$$r_{9,c9} = [r_f \;\; 0 \;\; 0]^T$$
$$r_{9,c8} = [0 \;\; 0 \;\; 0]^T$$
$$r_{10,c9} = [r_f - d_{\text{COP}} \;\; 0 \;\; 0]^T$$

where r_f is the distance of the CoM of the foot from the ankle/heel, and d_{COP} is the distance between the centre of pressure and the heel. The inertial properties of the foot are

$$m_f = 1.073 \text{ kg}$$

$$L_f = 0.2035 \text{ m}, \; r_f = 0.09 \text{ m}$$

$$\text{MI}_f = \begin{bmatrix} 0 & 0 & 0 \\ 0 & 0.01 & 0 \\ 0 & 0 & 0.01 \end{bmatrix} \text{ kg-m}^2$$

The joint moments are now computed, and their plots are shown in figures 3.23 to 3.28.

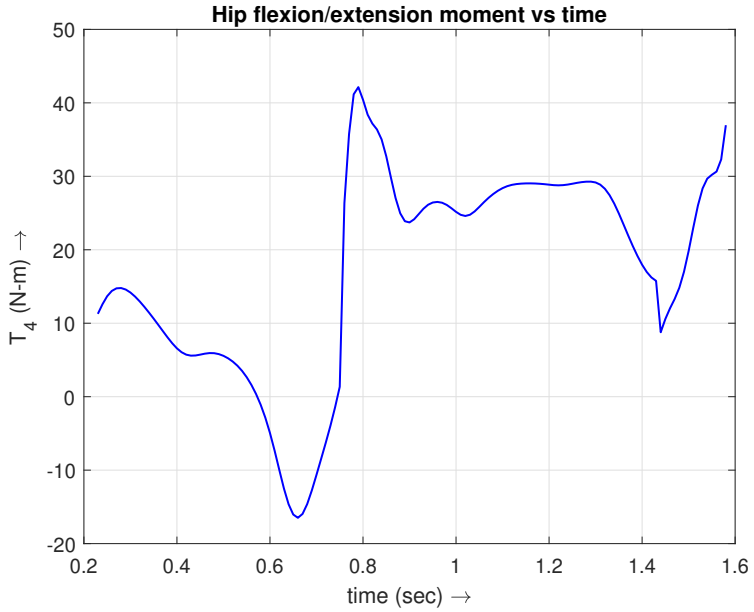

Figure 3.23: Variation of T_4 versus time

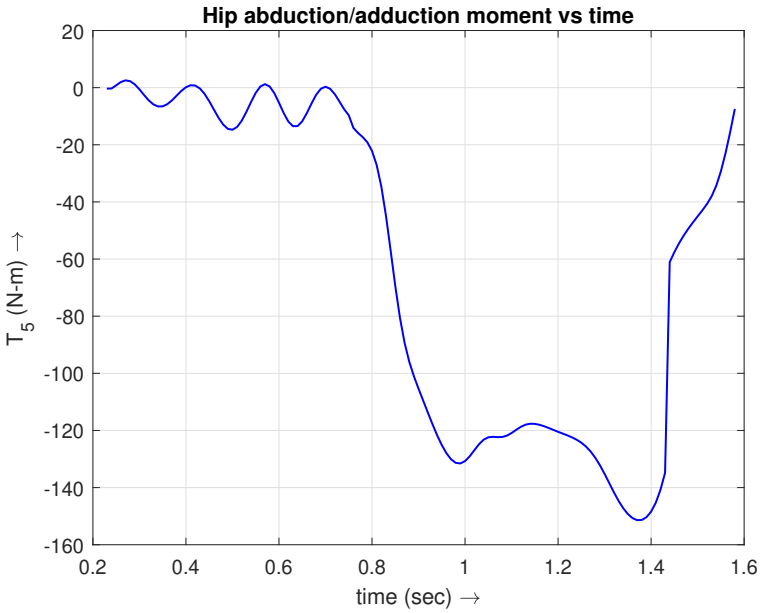

Figure 3.24: Variation of T_5 versus time

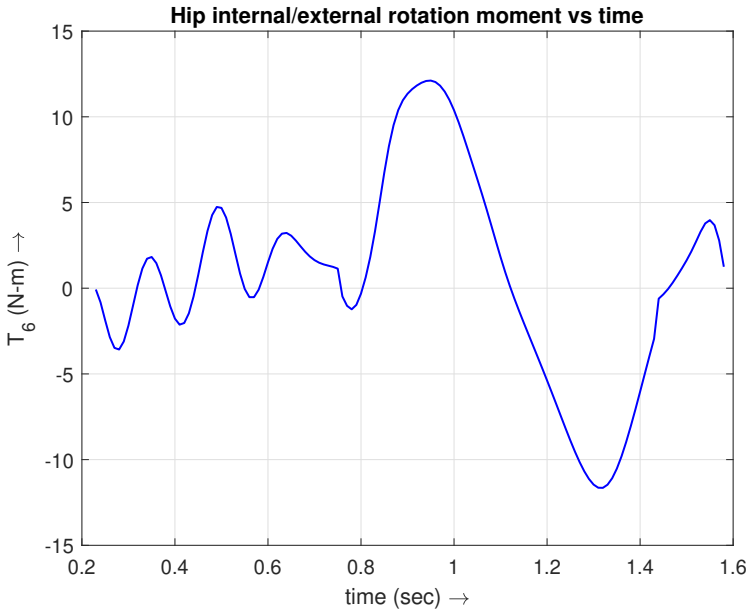

Figure 3.25: Variation of T_6 versus time

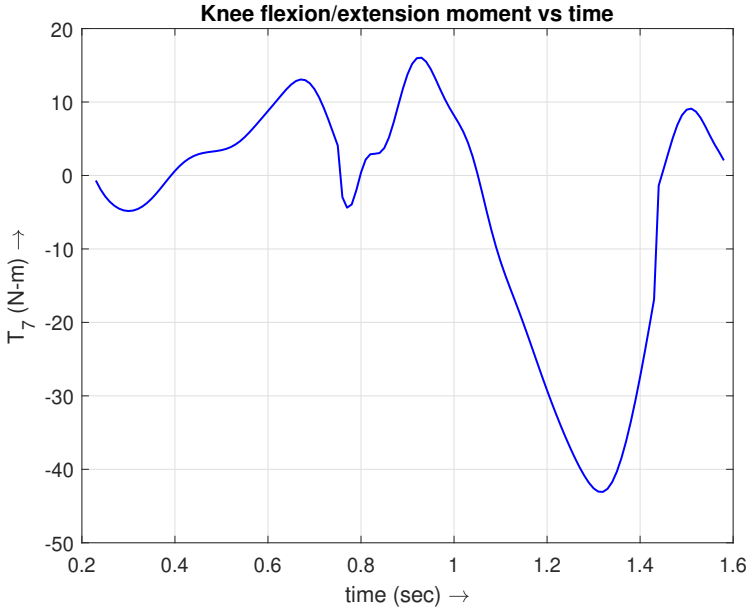

Figure 3.26: Variation of T_7 versus time

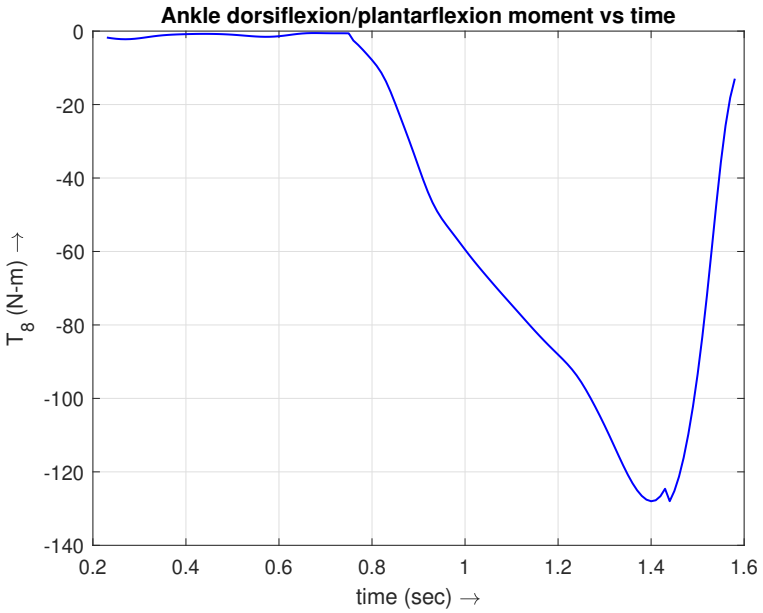

Figure 3.27: Variation of T_8 versus time

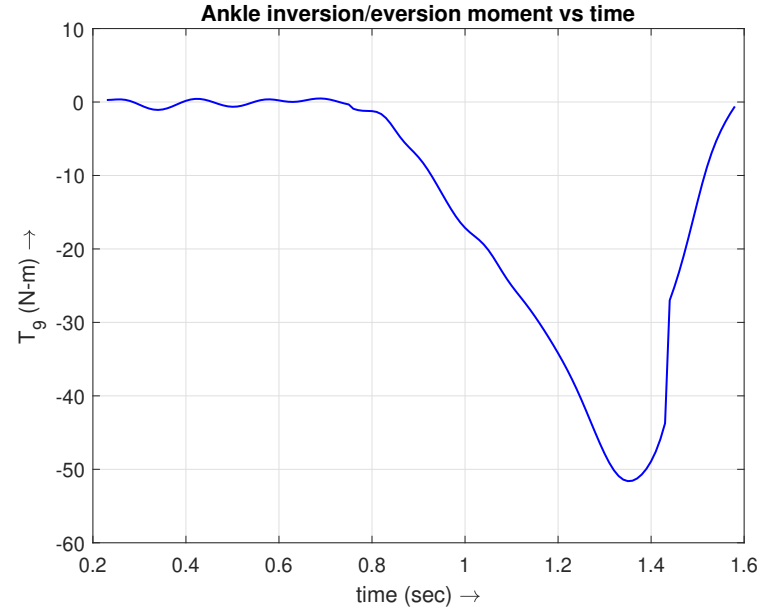

Figure 3.28: Variation of T_9 versus time

3.4 2D analysis without GRF prescribed

So far in all the analyses, we have assumed that data about the ground reaction forces is available, usually from force plate measurements. However in many situations, this data might just simply be unavailable, or it might be infeasible to measure it. Thus, the ground reaction forces need to be determined from the

kinematic data itself. We now present a novel formulation in which the ground reaction force is estimated from a lagrangian analysis and the zero-moment point (ZMP) concept. Walking is assumed to be a 2-dimensional activity, and all joints are assumed to be simple hinge joints. Typically, in double stance, the number of unknowns are more as compared to single stance because both the feet are in contact with the ground. To tackle this, in the formulation, both the feet are assumed to be like rollers, with effectively one point of contact, in the double stance phase. However in the single stance phase, the foot is approximated as a triangle, with effectively two points of contact with the ground. This ensures the number of unknowns remains the same throughout the analysis. This is illustrated in figure 3.29, which shows a 9 DOF model of human walking in 2D. The x-axis is in the direction of walking (AP axis), and the y-axis is along the longitudinal axis.

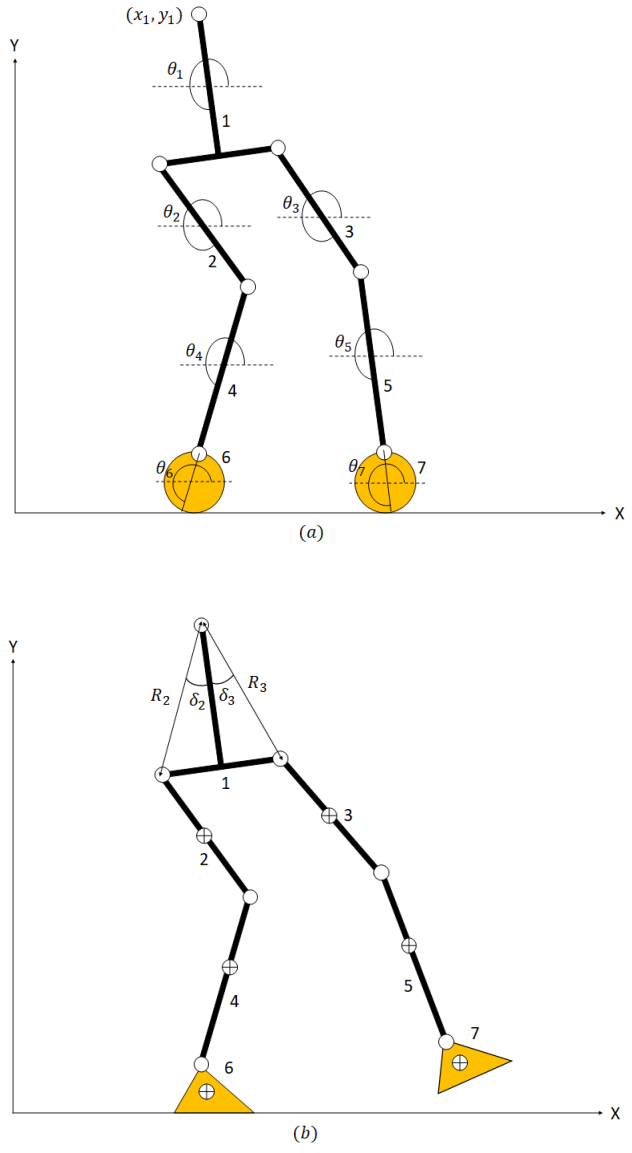

Figure 3.29: Nine DOF humanoid model for (a) double stance (b) single stance.

In this mechanism, link 1 is the trunk and pelvis, link 2 is the right thigh, link 3 is the left thigh, link 4 is the right shank, link 5 is the left shank, link 6 is the right foot, and link 7 is the left foot. Also θ_1 is the angle of trunk flexion, and θ_2, θ_4 and θ_6 are the angles made by the right thigh, shank and foot respectively, with the horizontal. Similarly θ_3, θ_5 and θ_7 are the angles made by the left thigh, shank and foot respectively, with the horizontal. Let the CoM of link i be at (x_i, y_i), for $1 \leq i \leq 7$, and L_i be the length of link i, for $2 \leq i \leq 7$. Let R_2 and R_3 be the distance from the CoM of link 1 to the right hip joint and left hip joint respectively. They are offset from the median line of link 1 by angles δ_2 and δ_3 respectively. The 9 DOF are

$$q = [x_1 \;\; y_1 \;\; \theta_1 \;\; \theta_2 \;\; \theta_3 \;\; \theta_4 \;\; \theta_5 \;\; \theta_6 \;\; \theta_7] \tag{3.64}$$

Let the coordinates of the right hip, knee and ankle be $(x_{\mathrm{rh}}, y_{\mathrm{rh}})$, $(x_{\mathrm{rk}}, y_{\mathrm{rk}})$ and $(x_{\mathrm{ra}}, y_{\mathrm{ra}})$ respectively. Similarly, the coordinates of the left hip, knee and ankle are denoted by $(x_{\mathrm{lh}}, y_{\mathrm{lh}})$, $(x_{\mathrm{lk}}, y_{\mathrm{lk}})$ and $(x_{\mathrm{la}}, y_{\mathrm{la}})$ respectively. The CoM of the pelvis is assumed to lie approximately on the mid-point of the line joining the right and left hip joints, and so its coordinates are given by

$$x_{\mathrm{p}} = \frac{x_{\mathrm{rh}} + x_{\mathrm{lh}}}{2}, \;\; y_{\mathrm{p}} = \frac{y_{\mathrm{rh}} + y_{\mathrm{lh}}}{2} \tag{3.65}$$

Since we know the coordinates of the trunk, hip, knee and ankle from the gait data, the angles can be estimated by

$$\theta_1 = \pi + \mathrm{atan2}(y_1 - y_{\mathrm{p}}, x_1 - x_{\mathrm{p}}) \tag{3.66}$$

$$\theta_2 = \pi + \mathrm{atan2}(y_{\mathrm{rh}} - y_{\mathrm{rk}}, x_{\mathrm{rh}} - x_{\mathrm{rk}}) \tag{3.67}$$

$$\theta_3 = \pi + \mathrm{atan2}(y_{\mathrm{lh}} - y_{\mathrm{lk}}, x_{\mathrm{lh}} - x_{\mathrm{lk}}) \tag{3.68}$$

$$\theta_4 = \pi + \mathrm{atan2}(y_{\mathrm{rk}} - y_{\mathrm{ra}}, x_{\mathrm{rk}} - x_{\mathrm{ra}}) \tag{3.69}$$

$$\theta_5 = \pi + \mathrm{atan2}(y_{\mathrm{lk}} - y_{\mathrm{la}}, x_{\mathrm{lk}} - x_{\mathrm{la}}) \tag{3.70}$$

$$\theta_6 = \pi + \mathrm{atan2}(y_{\mathrm{ra}} - y_6, x_{\mathrm{ra}} - x_6) \tag{3.71}$$

$$\theta_7 = \pi + \mathrm{atan2}(y_{\mathrm{la}} - y_7, x_{\mathrm{la}} - x_7) \tag{3.72}$$

The CoM locations of the links are now given by

$$x_2 = x_1 + R_2\cos(\theta_1 - \delta_2) + r_2\cos\theta_2 \tag{3.73}$$

$$y_2 = y_1 + R_2\sin(\theta_1 - \delta_2) + r_2\sin\theta_2 \tag{3.74}$$

$$x_3 = x_1 + R_3\cos(\theta_1 + \delta_3) + r_3\cos\theta_3 \tag{3.75}$$

$$y_3 = y_1 + R_3\sin(\theta_1 + \delta_3) + r_3\sin\theta_3 \tag{3.76}$$

$$x_4 = x_1 + R_2\cos(\theta_1 - \delta_2) + L_2\cos\theta_2 + r_4\cos\theta_4 \tag{3.77}$$

$$y_4 = y_1 + R_2\sin(\theta_1 - \delta_2) + L_2\sin\theta_2 + r_4\sin\theta_4 \tag{3.78}$$

$$x_5 = x_1 + R_3\cos(\theta_1 + \delta_3) + L_3\cos\theta_3 + r_5\cos\theta_5 \tag{3.79}$$

$$y_5 = y_1 + R_3\sin(\theta_1 + \delta_3) + L_3\sin\theta_3 + r_5\sin\theta_5 \tag{3.80}$$

$$x_6 = x_1 + R_2\cos(\theta_1 - \delta_2) + L_2\cos\theta_2 + L_4\cos\theta_4 + r_6\cos\theta_6 \tag{3.81}$$

$$y_6 = y_1 + R_2\sin(\theta_1 - \delta_2) + L_2\sin\theta_2 + L_4\sin\theta_4 + r_6\sin\theta_6 \tag{3.82}$$

$$x_7 = x_1 + R_3\cos(\theta_1 + \delta_3) + L_3\cos\theta_3 + L_5\cos\theta_5 + r_7\cos\theta_7 \tag{3.83}$$

$$y_7 = y_1 + R_3\sin(\theta_1 + \delta_3) + L_3\sin\theta_3 + L_5\sin\theta_5 + r_7\sin\theta_7 \tag{3.84}$$

We now compute the lagrangian $\mathcal{L}$, which is given by

$$\mathcal{L} = \sum_{i=1}^{7}\mathrm{KE}_i - \sum_{i=1}^{7}\mathrm{PE}_i + \mathrm{W}_{\mathrm{ext}} + \lambda_{\mathrm{n},1}h_{\mathrm{n},1} + \lambda_{\mathrm{n},2}h_{\mathrm{n},2} + \lambda_{\mathrm{t},1}h_{\mathrm{t},1} + \lambda_{\mathrm{t},2}h_{\mathrm{t},2} \tag{3.85}$$

where

$$\mathrm{KE}_i = \frac{1}{2}m_i(\dot{x}_i^2 + \dot{y}_i^2) + \frac{1}{2}\mathrm{MI}_i\dot{\theta}_i^2 \tag{3.86}$$

$$\mathrm{PE}_i = m_i g y_i \tag{3.87}$$

$$\mathrm{W}_{\mathrm{ext}} = \tau_2(\theta_2 - \theta_1) + \tau_3(\theta_3 - \theta_1) + \tau_4(\theta_4 - \theta_2) + \tau_5(\theta_5 - \theta_3) + \tau_6(\theta_6 - \theta_4) + \tau_7(\theta_7 - \theta_5) \tag{3.88}$$

Also, λ denotes the lagrange multipliers, i.e force at the corresponding contact, and h represent constraints corresponding to each contact. For double stance, they are given by

$$h_{\mathrm{n},1} = y_1 + R_2\sin(\theta_1 - \delta_2) + L_2\sin\theta_2 + L_4\sin\theta_4 + L_6\sin\theta_6 \tag{3.89}$$

$$h_{\mathrm{n},2} = y_1 + R_3\sin(\theta_1 + \delta_3) + L_3\sin\theta_3 + L_5\sin\theta_5 + L_7\sin\theta_7 \tag{3.90}$$

$$h_{t,1} = x_1 + R_2 \cos(\theta_1 - \delta_2) + L_2 \cos\theta_2 + L_4 \cos\theta_4 + L_6 \cos\theta_6 \tag{3.91}$$

$$h_{t,2} = x_1 + R_3 \cos(\theta_1 + \delta_3) + L_3 \cos\theta_3 + L_5 \cos\theta_5 + L_7 \cos\theta_7 \tag{3.92}$$

Note that in this situation, we have two contact points, one for each foot, each of which is modelled as a roller. For single stance of the right foot, they are given by

$$h_{n,1} = y_1 + R_2 \sin(\theta_1 - \delta_2) + L_2 \sin\theta_2 + L_4 \sin\theta_4 + r_6 \sin\theta_6 + r_{6b} \sin(\pi - \theta_6 + \gamma_{61}) \tag{3.93}$$

$$h_{n,2} = y_1 + R_2 \sin(\theta_1 - \delta_2) + L_2 \sin\theta_2 + L_4 \sin\theta_4 + r_6 \sin\theta_6 + r_{6f} \sin(\pi - \theta_6 + \gamma_{62}) \tag{3.94}$$

$$h_{t,1} = x_1 + R_2 \cos(\theta_1 - \delta_2) + L_2 \cos\theta_2 + L_4 \cos\theta_4 + r_6 \cos\theta_6 + r_{6b} \cos(\pi - \theta_6 + \gamma_{61}) \tag{3.95}$$

$$h_{t,2} = x_1 + R_2 \cos(\theta_1 - \delta_2) + L_2 \cos\theta_2 + L_4 \cos\theta_4 + r_6 \cos\theta_6 + r_{6f} \cos(\pi - \theta_6 + \gamma_{62}) \tag{3.96}$$

In this case, we have two contact points for the right foot, which is modelled as a triangle. The parameters in equations (3.93)-(3.96) are illustrated in figure 3.30.

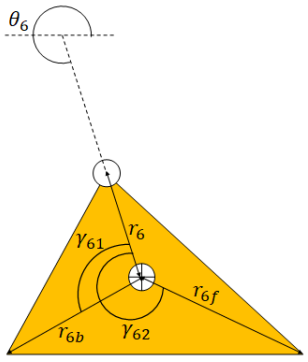

Figure 3.30: Right foot modelled as a triangle in single stance

Similarly, we can write expressions for the contact constraints for single stance of the left foot. Having computed the lagrangian, the lagrangian equations of motion are now given by

$$\frac{d}{dt}\left(\frac{\partial \mathcal{L}}{\partial \dot{q}_j}\right) - \frac{\partial \mathcal{L}}{\partial q_j} = 0, \qquad j = 1, 2, \ldots, 9 \tag{3.97}$$

This only gives us 9 equations, one for each DOF. Since we have 10 unknowns (6

joint torques and 4 lagrange multipliers), we require another equation. Hence, we use the ZMP equation, in which moments of all external and inertial forces are zero about the ZMP. According to [7] and [8], the ZMP is the projection of the CoM of the system on the floor. That is

$$x_{\text{ZMP}} = \frac{\sum_{i=1}^{7} m_i x_i}{\sum_{i=1}^{7} m_i}, \quad y_{\text{ZMP}} = 0 \tag{3.98}$$

The ZMP equation is then given by

$$\sum_{k=1}^{2}[h_{\text{n},k} - x_{\text{ZMP}}, 0] \otimes [0, \lambda_{\text{n},k}] - \sum_{i=1}^{7}[x_i - x_{\text{ZMP}}, y_i - y_{\text{ZMP}}] \otimes [m_i\ddot{x}_i, m_i(g + \ddot{y}_i)] - \sum_{i=1}^{7} \text{MI}_i\ddot{\theta}_i = 0 \tag{3.99}$$

where $\otimes$ denotes the 2D cross product. Thus we have 10 equations in 10 unknowns. The duration of different events of the gait cycle were outlined in table 2.2. Hence, the GRF in the x-direction for the right leg is given by

$$\text{GRF}_x = \begin{cases} 0 & 0.23 \leq t \leq 0.75 \\ \lambda_{\text{t},1} & 0.76 \leq t \leq 0.9 \\ \lambda_{\text{t},1} + \lambda_{\text{t},2} & 0.91 \leq t \leq 1.43 \\ \lambda_{\text{t},1} & 1.44 \leq t \leq 1.58 \end{cases} \tag{3.100}$$

Similarly, we have

$$\text{GRF}_y = \begin{cases} 0 & 0.23 \leq t \leq 0.75 \\ \lambda_{\text{n},1} & 0.76 \leq t \leq 0.9 \\ \lambda_{\text{n},1} + \lambda_{\text{n},2} & 0.91 \leq t \leq 1.43 \\ \lambda_{\text{n},1} & 1.44 \leq t \leq 1.58 \end{cases} \tag{3.101}$$

The inertial properties of the trunk are

$$m_1 = 50.172 \text{ kg}, \text{MI}_1 = 1.95 \text{ kg-m}^2$$

$$R_2 = 0.4028 \text{ m}, \; R_3 = 0.4061 \text{ m}, \; \delta_2 = 1.142^\circ, \; \delta_3 = 1.20^\circ$$

The inertial properties of the thigh, shank and foot are the same as the ones used in section 3.1. The GRF is computed from this formulation, and compared with experimental values that we have used before from [5]. This is illustrated in figures 3.31 and 3.32. The blue line denotes GRF computed from our formulation, and the red line denotes experimental GRF.

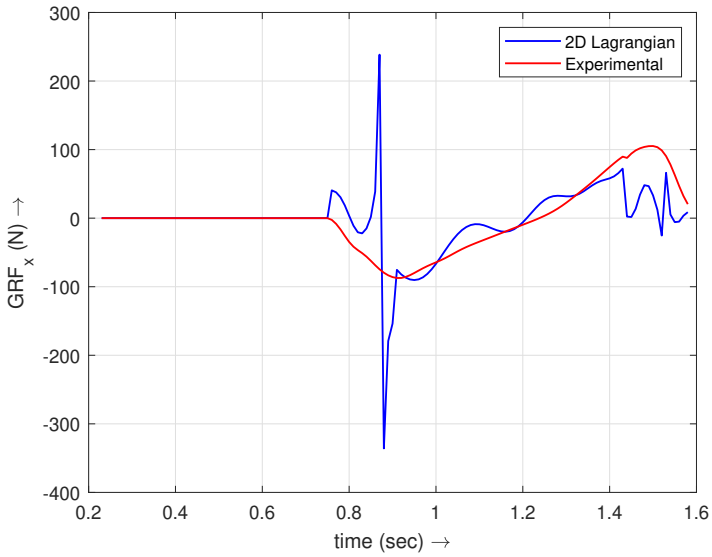

Figure 3.31: Plot of GRF_x versus time for one gait cycle

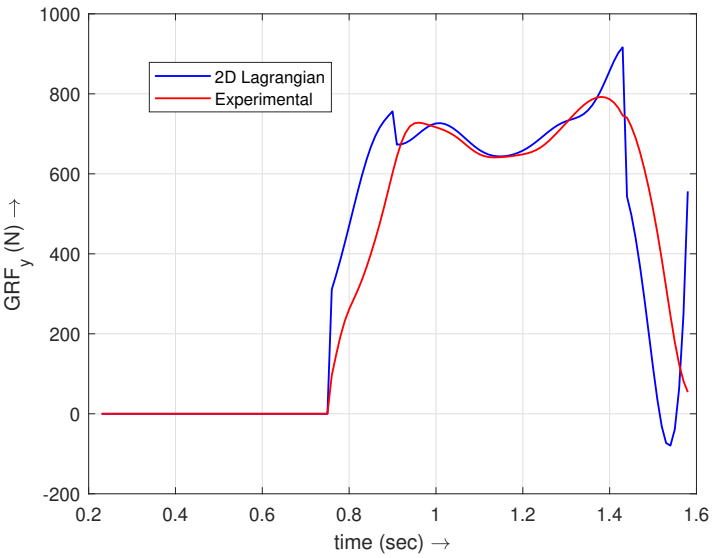

Figure 3.32: Plot of GRF_y versus time for one gait cycle

We can observe that there is good agreement between the experimental values, and the values calculated from the 2D lagrangian analysis. There are phases where the

values don't match, rather the calculated values are quite high for GRF_x between 0.8 and 0.9 sec. This is due to the coefficient matrix having near zero determinant in those phases. To address this, we propose to use experimental data for other healthy individuals from [5]. We assume the GRF in those regions to be a linear function of joint velocities and accelerations. The parameters of this function are then estimated using regression techniques. Let

$$Q = [\dot{q} \;\; \ddot{q}] \tag{3.102}$$

where q was defined in equation (3.64). Note that Q is a $N \times p$ matrix, where N is the number of observations, and p is the number of predictors (equal to 18). For regression, we use these 18 predictor variables, and our response variable is $Y = \text{GRF}_x$. We now say that

$$Y_i = c_0 + \sum_{j=1}^{p} c_j Q_{ij} + \epsilon_i \tag{3.103}$$

where ϵ_i is an error term for the i^{th} observation. There are three types of errors that are usually minimized to determine the coefficients c_j. They are

$$E_1 = \sum_{i=1}^{N} \left(Y_i - c_0 - \sum_{j=1}^{p} c_j Q_{ij} \right)^2 \tag{3.104}$$

$$E_2 = E_1 + \psi \sum_{j=1}^{p} c_j^2 \tag{3.105}$$

$$E_3 = E_1 + \psi \sum_{j=1}^{p} |c_j| \tag{3.106}$$

where ψ is a tunable parameter. The coefficients c_j that minimize E_1, E_2 and E_3 correspond to linear regression, ridge regression, and the lasso respectively. However, coefficient estimates for linear regression rely on the independence of the predictor variables. If the terms are correlated and the columns of the matrix Q have an approximate linear dependence, then the estimates are highly sensitive to random errors in the observed response Y, and their variance increases. Hence, we use ridge regression and the lasso, as it allows us to estimate coefficients even if we have linearly correlated predictors. Minimizing the penalty term in equations (3.105) and (3.106) has the effect of shrinking some coefficient estimates towards

zero. Hence both ridge regression and the lasso perform predictor selection. The predictor having a very small coefficient estimate has little to no effect on Y. More details about ridge regression and the lasso can be found in [2].

We use the gait data and force plate data for other healthy individuals, which is essentially our training set, to estimate the coefficients c_j in equation (3.103) by minimizing E_2 and E_3. After this, we find

$$\hat{Y}_i = c_0 + \sum_{j=1}^{p} c_j \tilde{Q}_{ij} \tag{3.107}$$

where $\tilde{Q}_{ij}$ are the joint velocities and accelerations of the candidate whose GRF is to be estimated. This is basically our test set. Note that we assume this linear dependence (equation (3.103)) only in regions where GRF_x calculated from the 2D lagrangian analysis do not match with experimental values. We thus use equation (3.107) to estimate GRF_x in these same regions. We do a similar analysis for GRF_y, and so are able to determine both GRF_x and GRF_y over the entire range of the gait cycle. Their plots are now shown in figures 3.33 and 3.34.

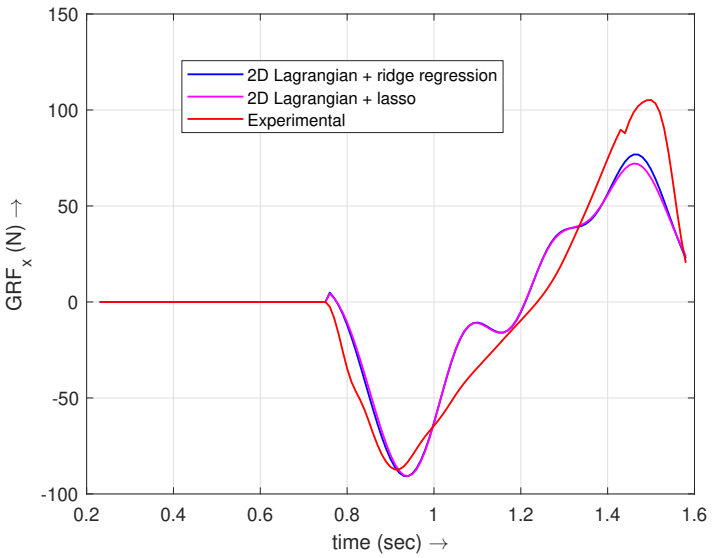

Figure 3.33: Plot of GRF_x versus time for one gait cycle

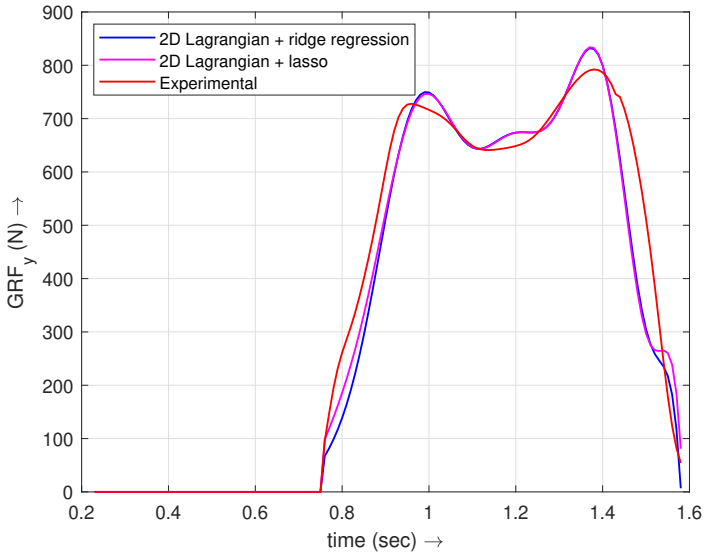

Figure 3.34: Plot of GRF_y versus time for one gait cycle

The blue line denotes GRF computed from ridge regression, the magenta line denotes GRF computed from the lasso, and the red line denotes experimental GRF. We can observe excellent agreement between the calculated and experimental values, over the entire gait cycle. Now that the GRF is determined, we can compute the joint moments from section 3.1. We will also compute them at the end of section 3.5.

3.5 3D analysis without GRF prescribed

We now perform a whole-body analysis in 3D to estimate the ground reaction forces. Consider a 16 DOF model of a humanoid. Here, 1 DOF is due to trunk flexion in the sagittal plane. The hip joint is a ball and socket joint with 3 DOF, the knee joint is a simple hinge joint with 1 DOF, and the ankle joint has 2 DOF. We use algorithm 1 to assign coordinate frames to the mechanism. This is illustrated in figure 3.35.

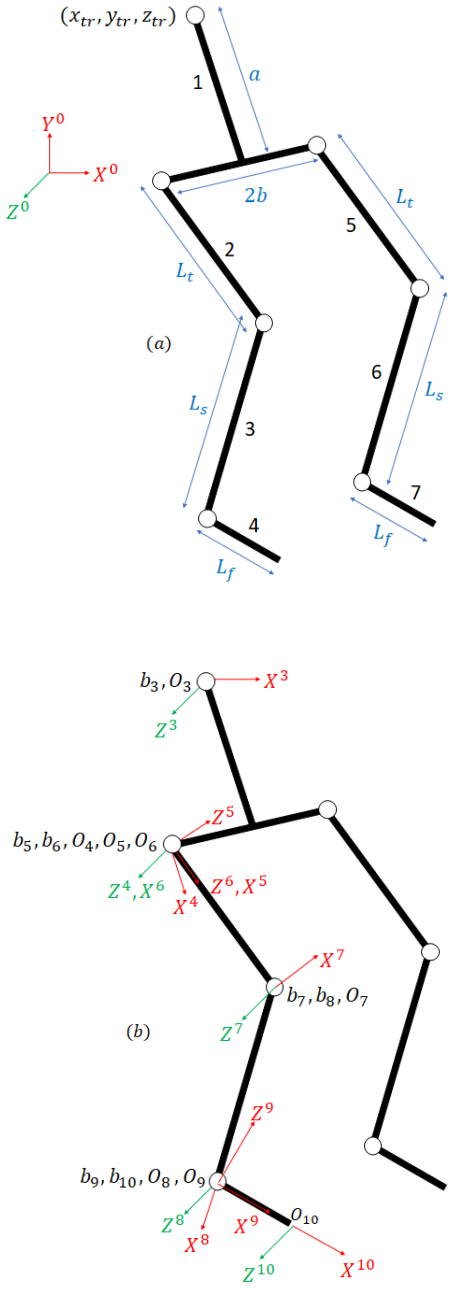

Figure 3.35: (a) Model of the 16 DOF humanoid (b) Assignment of coordinate frames as per algorithm 1 (shown only for the right side).

As in section 3.2, the X^0 axis is along the AP axis, the Y^0 axis is along the longitudinal axis, and the Z^0 axis is along the ML axis. The trunk is assumed to be brought to the coordinates $(x_{\text{tr}}, y_{\text{tr}}, z_{\text{tr}})$ by three prismatic joints, and so the assignment of the first 3 frames is exactly similar to the previous 3D analysis done in sections 3.2 and 3.3. Hence the first 3 frames have not been shown here. The frame assignment is only shown for the right side, but is done in a very similar manner for the left side. The DH parameters for this mechanism are tabulated in tables 3.3 and 3.4.

Table 3.3: DH parameters for the right side in figure 3.35

Axis	ϕ_i	d_i	a_i	β_i
$i = 1$	$\pi/2$	z_{tr}	0	$\pi/2$
$i = 2$	$\pi/2$	x_{tr}	0	$\pi/2$
$i = 3$	$\pi/2$	y_{tr}	0	$\pi/2$
$i = 4$	θ_1	b	a	0
$i = 5$	θ_2	0	0	$-\pi/2$
$i = 6$	θ_3	0	0	$-\pi/2$
$i = 7$	θ_4	L_t	0	$-\pi/2$
$i = 8$	θ_5	0	L_s	0
$i = 9$	θ_6	0	0	$-\pi/2$
$i = 10$	θ_7	0	L_f	$\pi/2$

Table 3.4: DH parameters for the left side in figure 3.35

Axis	ϕ_i	d_i	a_i	β_i
$i = 1$	$\pi/2$	z_{tr}	0	$\pi/2$
$i = 2$	$\pi/2$	x_{tr}	0	$\pi/2$
$i = 3$	$\pi/2$	y_{tr}	0	$\pi/2$
$i = 4$	θ_1	$-b$	a	0
$i = 5$	θ_8	0	0	$-\pi/2$
$i = 6$	θ_9	0	0	$-\pi/2$
$i = 7$	θ_{10}	L_t	0	$-\pi/2$
$i = 8$	θ_{11}	0	L_s	0
$i = 9$	θ_{12}	0	0	$-\pi/2$
$i = 10$	θ_{13}	0	L_f	$\pi/2$

As usual, L_t, L_s and L_f are the lengths of the thigh, shank and foot respectively. The distance between the CoM of the trunk and CoM of the pelvis is a, and the length of the pelvis is $2b$. Angle θ_1 characterizes trunk flexion. For the right side, angles θ_2, θ_3 and θ_4 characterize flexion/extension, abduction/adduction and

internal/external rotation at the hip, respectively. Knee flexion/extension is characterized by angle θ_5, and ankle dorsiflexion/plantarflexion and inversion/eversion are characterized by angles θ_6 and θ_7 respectively. Similarly, we have angles θ_8, θ_9, θ_{10}, θ_{11}, θ_{12} and θ_{13} for the left side. Since we know the coordinates of the trunk, hip, knee, ankle and forefoot from the gait data, all these angles are estimated using inverse kinematics.

As is clear from figure 3.35, for the mechanism, link 1 is the trunk and pelvis, link 2 is the right thigh, link 3 is the right shank, link 4 is the right foot, link 5 is the left thigh, link 6 is the left shank and link 7 is the left foot. Let the CoM of link i be located at (x_i, y_i, z_i) in the ground frame of reference (frame 0). Note that $x_1 = x_{\text{tr}}$, $y_1 = y_{\text{tr}}$, and $z_1 = z_{\text{tr}}$. We now wish to get expressions for these coordinates. If we know the CoM location of a particular link with respect to some other frame of reference, we can use an appropriate transformation matrix to get the CoM coordinates in the base frame. For example, the CoM location of link 2 with respect to frame 7 is $[0 \;\; L_t - r_t \;\; 0]^T$. Thus we have

$$\begin{bmatrix} x_2 \\ y_2 \\ z_2 \\ 1 \end{bmatrix} = T_7^0 \begin{bmatrix} 0 \\ L_t - r_t \\ 0 \\ 1 \end{bmatrix} \tag{3.108}$$

This gives us

$$x_2 = x_{\text{tr}} + a\cos\theta_1 - r_t \sin\theta_3 \cos(\theta_1 + \theta_2) \tag{3.109}$$

$$y_2 = y_{\text{tr}} + a\sin\theta_1 - r_t \sin\theta_3 \sin(\theta_1 + \theta_2) \tag{3.110}$$

$$z_2 = z_{\text{tr}} + b - r_t \cos\theta_3 \tag{3.111}$$

Similarly, we can get CoM locations of the other links as well.

Let $m_{\text{tot}} = \sum_{i=1}^{7} m_i$, where m_i is the mass of link i. We can now get expressions for the acceleration of the CoM of the system by

$$\ddot{x}_{\text{CoM}} = \frac{\sum_{i=1}^{7} m_i \ddot{x}_i}{m_{\text{tot}}} \tag{3.112}$$

$$\ddot{y}_{\text{CoM}} = \frac{\sum_{i=1}^{7} m_i \ddot{y}_i}{m_{\text{tot}}} \tag{3.113}$$

$$\ddot{z}_{\text{CoM}} = \frac{\sum_{i=1}^{7} m_i \ddot{z}_i}{m_{\text{tot}}} \tag{3.114}$$

The only external forces that act during walking are the ground reaction forces and gravity. Therefore in the single stance phase, where only one foot contacts the ground, the equations of motions give

$$\text{GRF}_x = m_{\text{tot}} \ddot{x}_{\text{CoM}} \tag{3.115}$$

$$\text{GRF}_y = m_{\text{tot}} \ddot{y}_{\text{CoM}} + m_{\text{tot}} g \tag{3.116}$$

$$\text{GRF}_z = m_{\text{tot}} \ddot{z}_{\text{CoM}} \tag{3.117}$$

Thus the GRF in single stance phase can be determined from these equations. However in the double stance phase, where both feet contact the ground, the equations of motion now give

$$\text{GRF}_x^R + \text{GRF}_x^L = m_{\text{tot}} \ddot{x}_{\text{CoM}} \tag{3.118}$$

$$\text{GRF}_y^R + \text{GRF}_y^L = m_{\text{tot}} \ddot{y}_{\text{CoM}} + m_{\text{tot}} g \tag{3.119}$$

$$\text{GRF}_z^R + \text{GRF}_z^L = m_{\text{tot}} \ddot{z}_{\text{CoM}} \tag{3.120}$$

where GRF^R and GRF^L denote the GRF due to the right and left foot, respectively. Unlike the situation in single stance, we cannot solve these equations for the GRF as we have 3 equations for 6 unknowns. To address this, we again make use of the ZMP concept. Like in our previous 2D lagrangian analysis, the ZMP is the projection of the CoM of the system on the floor ([7] and [8]). That is, it has the coordinates $(x_{\text{CoM}}, 0, z_{\text{CoM}})$, where

$$x_{\text{CoM}} = \frac{\sum_{i=1}^{7} m_i x_i}{m_{\text{tot}}} \tag{3.121}$$

$$z_{\text{CoM}} = \frac{\sum_{i=1}^{7} m_i z_i}{m_{\text{tot}}} \tag{3.122}$$

Let v^R and v^L be vectors from the ZMP to the centres of the right and left foot respectively. We make an assumption that GRF_z is negligible in comparison to both GRF_x and GRF_y for either foot, which is a fairly accurate approximation. The two ZMP equations are thus given by (adapted from [8]):

$$v_z^R \text{GRF}_x^R + v_z^L \text{GRF}_x^L = 0 \tag{3.123}$$

$$v_x^R \text{GRF}_y^R + v_x^L \text{GRF}_y^L = 0 \tag{3.124}$$

These equations together with equations (3.118)-(3.119) give us the ground reaction forces. We now compare them with experimental values. The plots illustrating these are shown in figures 3.36 and 3.37. The blue line denotes GRF computed from this whole body analysis of the humanoid, and the red line denotes experimental GRF.

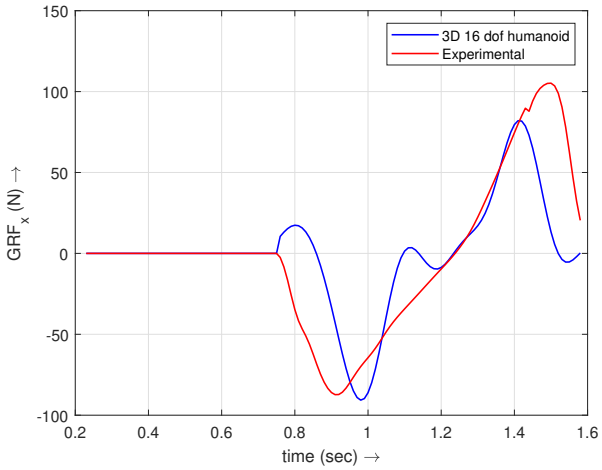

Figure 3.36: Plot of GRF_x versus time for one gait cycle

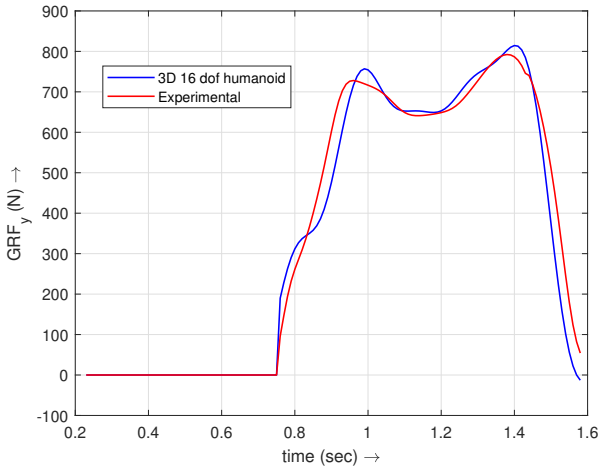

Figure 3.37: Plot of GRF_y versus time for one gait cycle

We observe that there is good agreement between the calculated and experimental values. We can now compute the joint moments by applying algorithm 2 and algorithm 3 for the 16 DOF humanoid. The GRF determined in this section, or from section 3.4, can be used in this computation. Note that in both these cases, we are assuming GRF_z to be negligible. The plots of the joint moments are shown in figures 3.38 to 3.43.

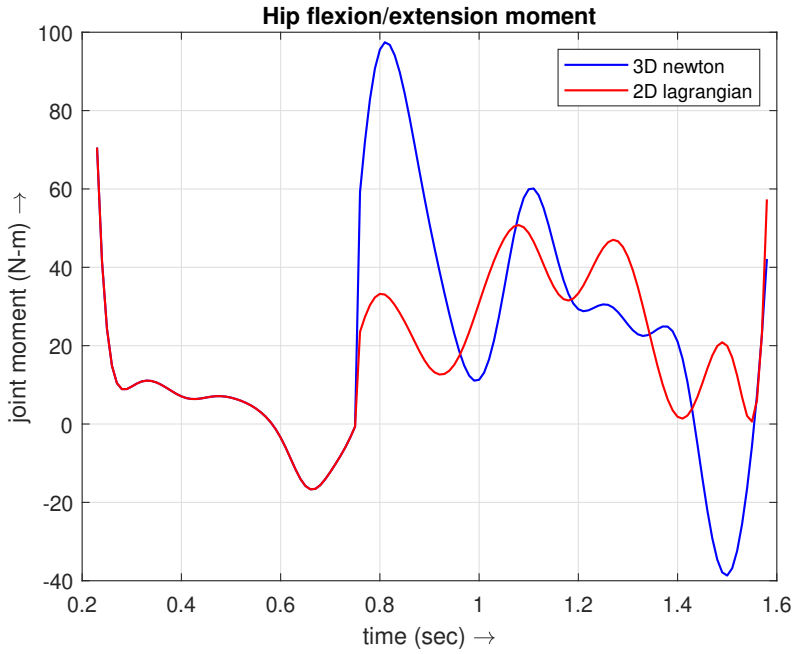

Figure 3.38: Variation of hip flexion/extension moment

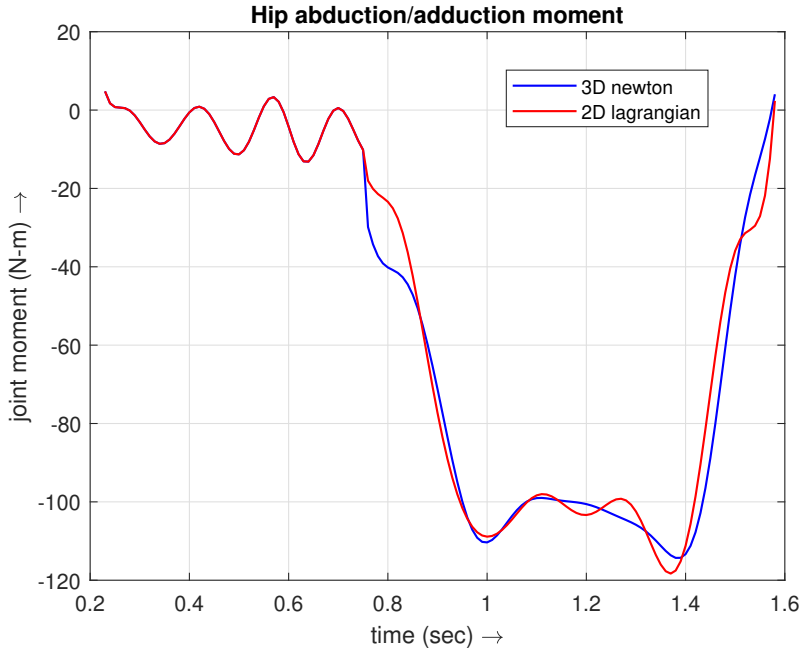

Figure 3.39: Variation of hip abduction/adduction moment

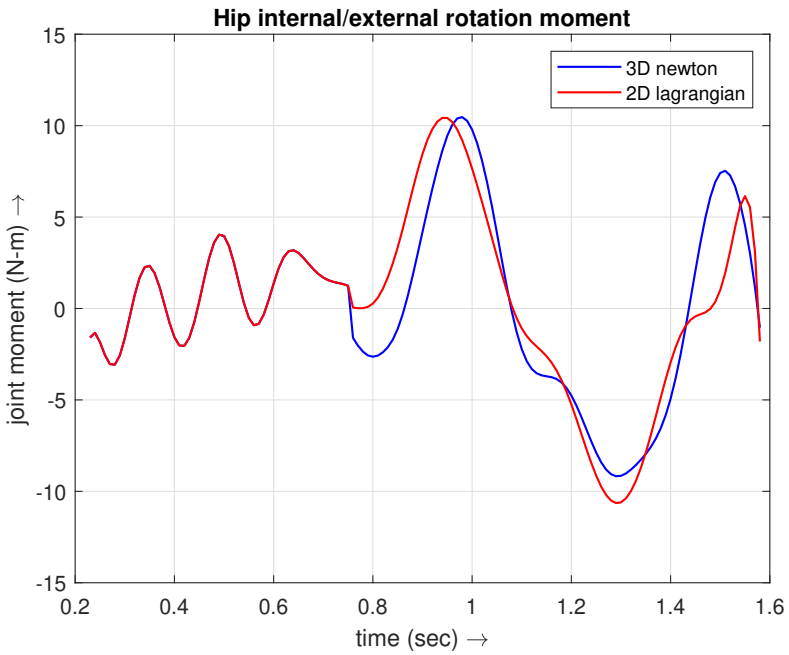

Figure 3.40: Variation of hip internal/external rotation moment

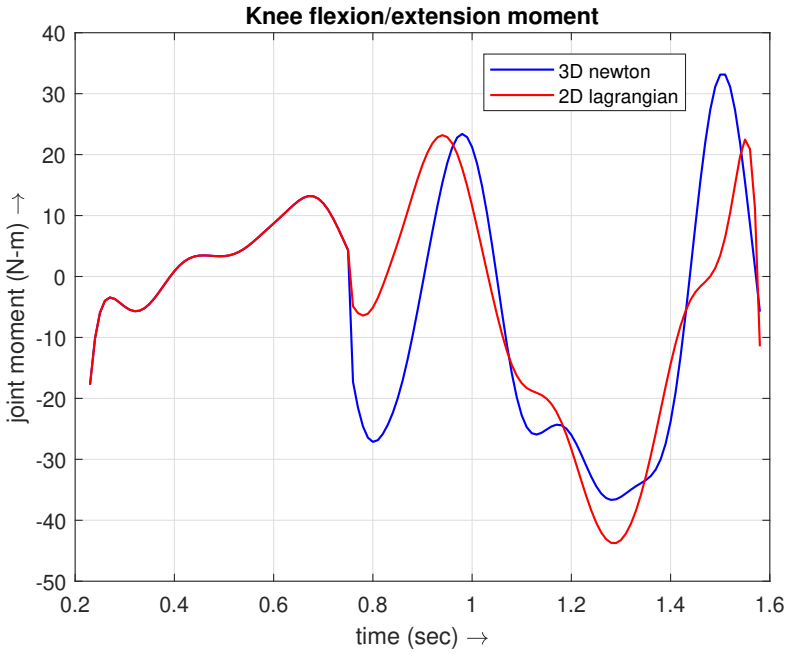

Figure 3.41: Variation of knee flexion/extension moment

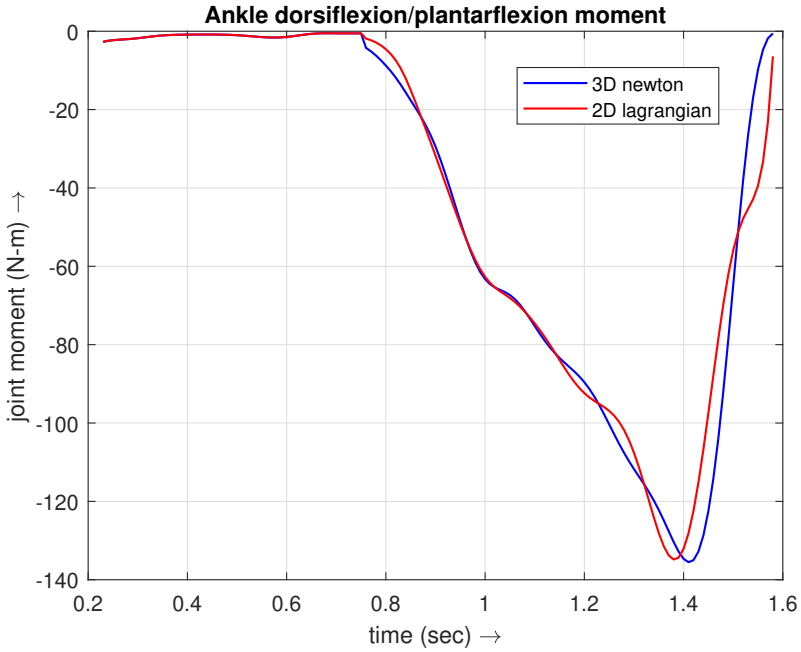

Figure 3.42: Variation of ankle dorsiflexion/plantarflexion moment

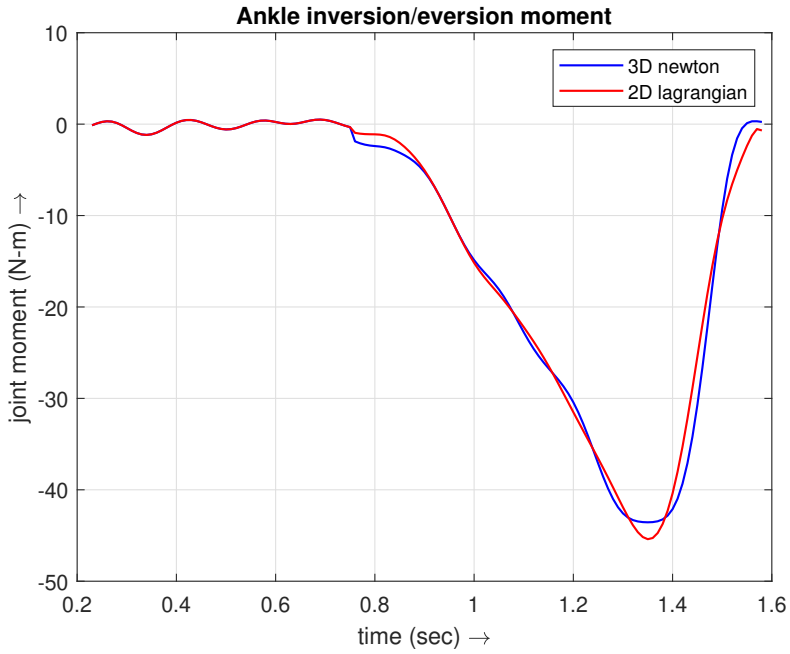

Figure 3.43: Variation of ankle inversion/eversion moment

The blue line denotes moments computed using GRF determined in this section, and the red line denotes moments computed using GRF determined in section 3.4. Therefore in this chapter, we have estimated joint moments for normal and healthy walking by carrying out inverse dynamics analyses in both 2D and 3D. We initially looked at situations where the GRF was known from force plate measurements. We

then investigated the case where the GRF was not known. For this, we calculated the GRF from the gait data itself, before finally computing the joint moments.

CHAPTER 4

CONCLUSION

Exoskeletons are wearable machines that help people, usually suffering from stroke or spinal cord injuries, regain their ability to walk. They correct the gait of the patient by applying moments corresponding to normal, healthy walking, at their joints. These moments are estimated by carrying out an inverse dynamics analysis for a healthy individual. This analysis generally requires (i) gait data (ii) ground reaction forces (GRF), and (iii) data about masses of the body segments and locations of their centre of mass. Gait data is easily collected using human motion capture systems, and information about body segment parameters is available from anthropometric data. In some cases, GRF data might be collected from force plate measurements. Thus, we started performing inverse dynamics analyses in which the GRF was known. We looked at a 2D model which had the thigh, shank and foot. We then moved to a 3D model which just had a thigh and shank, and derived important results. It was then extended to a model that had the foot as well. The joint moments were calculated for all of these cases, and were subsequently plotted.

It is important to realize that in many situations, GRF data might not be available, or it might be impractical or expensive to measure it. Hence we have to compute the GRF from just the gait data, and without relying on separate measurements from force plates. This necessitates a whole body analysis. We presented a novel formulation in which the ground reaction force was estimated from a 2D lagrangian analysis for the entire body, and the zero-moment point (ZMP) concept. The formulation ensured that the number of unknowns remained the same in both the double stance and single stance phases. The GRF computed from this method was then compared with experimental values. There was good agreement between the values, however there were regions where the values were not matching. We then assumed the GRF in those regions to be a function of joint velocities and accelerations. The parameters of this function were then estimated using regression techniques. We then also performed a whole body analysis for a 3D humanoid,

and together with the ZMP equation and the assumption that the GRF in the mediolateral direction is negligible, estimated the GRF.

Once the GRF is determined from either method, we can perform an analysis very similar to that carried out in section 3.3 to compute the joint moments. The motors of the exoskeleton can then apply these values of moments to correct the gait of the patient.

APPENDIX A

Mathematica Codes

1. `InverseDynamics2D.nb`

   Determines symbolic expressions of the joint moments in section 3.1.

2. `InverseDynamics3D-I.nb`

   Inverse kinemtics and determines symbolic expressions of the joint moments in section 3.2.

3. `InverseDynamics3D-II.nb`

   Inverse kinematics and determines symbolic expressions of the joint moments in section 3.3.

4. `HumanoidLag2D-DS.nb`

   Evaluates the lagrangian for the 9 DOF humanoid in section 3.4, and determines the coefficient matrix for the unknowns in the double stance phase.

5. `HumanoidLag2D-SS1.nb`

   Evaluates the lagrangian for the 9 DOF humanoid in section 3.4, and determines the coefficient matrix for the unknowns in the right leg single stance phase.

6. `HumanoidLag2D-SS2.nb`

   Evaluates the lagrangian for the 9 DOF humanoid in section 3.4, and determines the coefficient matrix for the unknowns in the left leg single stance phase.

7. `Humanoid3D-GRF.nb`

   Evaluates GRF for the 16 DOF humanoid in section 3.5.

APPENDIX B

MATLAB Codes

1. `InverseDynamics2D.m`

   Computes and plots the joint moments in section 3.1 using function `torques2D.m`.

2. `InverseDynamics3D_I.m`

   Computes and plots the joint moments in section 3.2 using function `torques3D_I.m`.

3. `InverseDynamics3D_II.m`

   Computes and plots the joint moments in section 3.3 using function `torques3D_II.m`.

4. `Humanoid2D_lag.m`

   Computes and plots GRF for the 9 DOF humanoid in section 3.4 using functions `double_stance_lag.m` (for double stance), `single_stance_r_lag.m` (for right leg single stance) and `single_stance_l_lag.m` (for left leg single stance).

5. `ts1.m ts2.m ..... ts6.m`

   Gait data and GRF data for 6 healthy individuals.

6. `Ridge_lasso_GRF.m`

   Evaluates coefficients for ridge regression and the lasso from the 6 training sets.

7. `Humanoid2D_lag_regression.m`

   Evaluates GRF for the particular individual using coefficients corresponding to ridge regression and the lasso.

8. `Humanoid3D_GRF_moments.m`

   Computes and plots GRF for the 16 DOF humanoid in section 3.5 using functions `double_stance_GRF.m` (for double stance) and `single_stance_GRF.m` (for single stance). It then computes and plots the joint moments using the function `torquesHumanoid3D.m`.

REFERENCES

[1] **Craig, J.**, *Introduction to Robotics: Mechanics and Control*. Pearson Education Limited, 2014.

[2] **James, G.**, **D. Witten**, **T. Hastie**, and **R. Tibshirani**, *An Introduction to Statistical Learning with Applications in R*. Springer Texts in Statistics, 2017.

[3] **Kirtley, C.**, *Clinical Gait Analysis: Theory and Practice*. Elsevier, 2006.

[4] **Schilling, R.**, *Fundamentals of Robotics: Analysis and Control*. Prentice-Hall of India Private Limited, 2003.

[5] **Schreiber, C.** and **F. Moissenet** (2019). A multimodal dataset of human gait at different walking speeds established on injury-free adult participants. *Scientific Data*, **6**(111).

[6] **Spong, M.**, **S. Hutchinson**, and **M. Vidyasagar**, *Robot Modeling and Control, Second Edition*. John Wiley & Sons Ltd, 2020.

[7] **Vukobratovic, M.** and **B. Borovac** (2004). Zero-moment point - thirty five years of its life. *International Journal of Humanoid Robotics*, **1**(1), 157–173.

[8] **Vukobratovic, M.**, **B. Borovac**, **D. Surla**, and **D. Stokic**, *Biped Locomotion: Dynamics, Stability, Control and Application*. Springer-Verlag, 1990.

[9] **Whittle, M.**, *Gait Analysis: An Introduction, Fourth Edition*. Elsevier, 2007.

LIST OF PAPERS BASED ON THESIS

1. Abhyudit Singh Manhas, Mowbray Rajagopalan and Dr. Sourav Rakshit A 2D Unified Gait Model for both single and double stances *The 6th Joint International Conference on Multibody System Dynamics and The 10th Asian Conference on Multibody System Dynamics* (in progress).